

This discussion paper is/has been under review for the journal *Atmospheric Chemistry and Physics (ACP)*. Please refer to the corresponding final paper in *ACP* if available.

**High-RH
hygroscopicity**

C. R. Ruehl et al.

Aerosol hygroscopicity at high (99 to 100%) relative humidities

C. R. Ruehl¹, P. Y. Chuang¹, and A. Nenes²

¹Earth & Planetary Sciences, University of California, Santa Cruz, USA

²Earth & Atmospheric Sciences, Georgia Institute of Technology, Atlanta, USA

Received: 14 July 2009 – Accepted: 14 July 2009 – Published: 24 July 2009

Correspondence to: C. R. Ruehl (crruehl@ucdavis.edu)

Published by Copernicus Publications on behalf of the European Geosciences Union.

Title Page

Abstract

Introduction

Conclusions

References

Tables

Figures

◀

▶

◀

▶

Back

Close

Full Screen / Esc

Printer-friendly Version

Interactive Discussion



Abstract

The hygroscopicity of an aerosol largely determines its influence on climate and, for smaller particles, atmospheric lifetime. While much aerosol hygroscopicity data is available at lower relative humidities (RH) and under cloud formation conditions (RH>100%), relatively little data is available at high RH (99.2 to 99.9%). We measured the size of droplets at high RH that had formed on particles composed of one of seven compounds with dry diameters between 0.1 and 0.5 μm , and calculated the hygroscopicity of these compounds. We use a parameterization of the Kelvin term, in addition to a standard parameterization (κ) of the Raoult term, to express the hygroscopicity of surface-active compounds.

For inorganic compounds, hygroscopicity could reliably be predicted using water activity data and assuming a surface tension of pure water. In contrast, most organics exhibited a slight to mild increase in hygroscopicity with droplet diameter. This trend was strongest for sodium dodecyl sulfate (SDS), the most surface-active compound studied. The results suggest that partitioning of surface-active compounds away from the bulk solution, which reduces hygroscopicity, dominates any increases in hygroscopicity due to reduced surface tension. This is opposite to what is typically assumed for soluble surfactants. Furthermore, we saw no evidence that micellization limits SDS activity in micron-sized solution droplets, as observed in macroscopic solutions. These results suggest that while the high-RH hygroscopicity of inorganic compounds can be reliably predicted using readily available data, surface-activity parameters obtained from macroscopic solutions with organic solutes may be inappropriate for calculations of the hygroscopicity of micron-sized droplets.

1 Introduction

Several mechanisms by which aerosols affect climate have been the subject of a great deal of recent study. These have broadly been classified as direct effects, in which

High-RH hygroscopicity

C. R. Ruehl et al.

Title Page

Abstract

Introduction

Conclusions

References

Tables

Figures

◀

▶

◀

▶

Back

Close

Full Screen / Esc

Printer-friendly Version

Interactive Discussion



High-RH hygroscopicity

C. R. Ruehl et al.

Title Page

Abstract

Introduction

Conclusions

References

Tables

Figures

◀

▶

◀

▶

Back

Close

Full Screen / Esc

Printer-friendly Version

Interactive Discussion



particles interact directly with radiation, or indirect effects, in which variation in aerosol properties cause changes in cloud properties that can have a substantial impact on climate. The magnitude of both direct and indirect effects depends strongly on aerosol hygroscopicity (roughly speaking, the amount of water absorbed by a particle at a given relative humidity, or RH). Particles that effectively absorb water at elevated RH have much larger scattering cross-sectional areas than less hygroscopic particles, and are also much more likely to act as cloud condensation nuclei (CCN), allowing them to indirectly affect climate. Accurate assessment of the effects of aerosols on climate therefore requires a detailed description of their hygroscopicities. In addition, wet deposition is the most efficient removal mechanism for particles with dry diameters ($D_{\text{dry}} < 1 \mu\text{m}$) (Textor et al., 2006), and therefore hygroscopicity and CCN activity strongly influence particle lifetime and thus total aerosol burden.

Aerosol hygroscopicity is controlled by two chemical properties of the compounds present in a particle: their ability to lower the water activity (a_w) of an aqueous solution, and their ability to lower the surface tension (σ) of the droplet-air interface. Accordingly, these two variables appear in the Köhler equation, which relates the ambient RH in equilibrium with a droplet to various droplet properties:

$$\text{RH} = a_w \exp\left(\frac{4\sigma\bar{V}_w}{RTD_{\text{wet}}}\right) \quad (1)$$

Here \bar{V}_w is the molar volume of the droplet (assumed to be equal to that of pure water), R is the gas constant, T is temperature, and D_{wet} is the droplet diameter. The influence on hygroscopicity of a_w and the exponential term containing σ are known as the Raoult and the Kelvin effects, respectively. The sensitivity of D_{wet} to these variables can be defined as the ratio of the resulting fractional change in D_{wet} to a small fractional change in either variable. Thus, the dimensionless sensitivity of D_{wet} to changes in a_w

is expressed as:

$$\frac{d\tilde{D}_{\text{wet}}}{d\tilde{a}_w} = \frac{dD_{\text{wet}}}{da_w} \times \frac{a_{w,0}}{D_{\text{wet},0}} \quad (2)$$

at some reference wet diameter ($D_{\text{wet},0}$) with a corresponding water activity ($a_{\text{wet},0}$). The sensitivity of D_{wet} to σ can be defined analogously. To calculate these sensitivities, we assume a chemical composition (specifically, molar volume \bar{V} and extent of dissociation) for the dry particle, and that a_w equals the mole fraction of water in the droplet (i.e., the solution is ideal) and is therefore proportional to $D_{\text{wet},0}^{-3}$. Once these

assumptions are made, Eq. (1) can be used to solve for $\frac{d\tilde{D}_{\text{wet}}}{d\tilde{a}_w}$ and $\frac{d\tilde{D}_{\text{wet}}}{d\tilde{\sigma}}$. Figure 1 indicates these sensitivities for ammonium sulfate particles as a function of D_{wet} and RH.

It is apparent that the sensitivity of D_{wet} to a_w is always relatively high, increasing only slightly as both RH increases and D_{wet} decreases. In contrast, the sensitivity of D_{wet} to σ is a much stronger function of both D_{wet} and RH, and is only relatively high when RH \gtrsim 99% and $D_{\text{wet}} \lesssim 2 \mu\text{m}$. This is because the magnitude of the Kelvin effect approaches that of the Raoult effect as RH \rightarrow 100% (Lewis, 2008), and also due to the greater curvature of smaller droplets which increases the importance of the Kelvin effect.

Most measurements of water activity at high RH (>99%) have been made not of droplets with typical atmospheric sizes ($D_{\text{wet}} \sim 1 \mu\text{m}$), but rather of macroscopic solutions with both a flat aqueous-air interface and a much smaller surface:volume ratio, measurements made at RH > 99% recently using the LACIS instrument notwithstanding (Wex et al., 2005; Ziese et al., 2008; Niedermeier et al., 2008; Wex et al., 2009). (Henceforth we use the term “macroscopic” to describe these larger solutions with flat interfaces, in the same way that others have used the term “bulk”. We reserve the term “bulk” for the portion of the solution not along its surface.) Measurements of the hygroscopicity of larger droplets, typically with D_{wet} between 20 and 40 μm , have been made using electrodynamic balances (e.g., Chan et al., 2008). High-resolution diameter measurements have also been made of droplets with $D_{\text{wet}} \sim 3$ to 7 μm at high RH using optical tweezers (Hanford et al., 2008). However, as can be seen in Fig. 1b, smaller droplets

High-RH hygroscopicity

C. R. Ruehl et al.

Title Page

Abstract

Introduction

Conclusions

References

Tables

Figures

◀

▶

◀

▶

Back

Close

Full Screen / Esc

Printer-friendly Version

Interactive Discussion



contain more information regarding the influence of surface-active (σ -lowering) solutes on aerosol hygroscopicity.

It has been argued that the surface activity of aerosols influences climate by reducing the surface tension of droplets relative to that of pure water droplets ($\sigma_{\text{H}_2\text{O}}=72.8 \text{ mJ m}^{-2}$ at 25°C). This would increase their hygroscopicity (particularly at high RH), resulting in higher cloud droplet concentrations and consequently greater cloud albedo (Facchini et al., 1999). Many studies have used the reduced σ measured in a macroscopic aqueous solution in calculations of aerosol particle hygroscopicity (e.g., Facchini et al., 1999; Dinar et al., 2006; Shulman et al., 1996; Hitzenberger et al., 2002; Asa-Awuku et al., 2008; Mircea et al., 2005; Lohmann and Leck, 2005; Rissman et al., 2004; Henning et al., 2005; Broekhuizen et al., 2004; Abdul-Razzak and Ghan, 2004). σ has often been measured using shape analysis of air bubbles in a sample cell with spatial dimensions of $20 \text{ mm} \times 20 \text{ mm} \times 40 \text{ mm}$ (e.g., Loglio et al., 1998; Facchini et al., 1999), which corresponds to a sample surface area:volume ratio of 250 m^{-1} . The bulk ring method, which requires $\sim 10 \text{ mL}$ of solution (e.g., Kiss et al., 2005), involves a similar surface:volume as the air bubble method. Recently Taraniuk et al. (2008) measured surface tension reduction in droplets with volumes $\sim 0.5 \text{ mL}$, or a surface:volume of $\sim 600 \text{ m}^{-1}$. Another commonly used technique (Shulman et al., 1996; Lima and Synovec, 1995; Varga et al., 2007; Dinar et al., 2007) involves measuring the volume of solution droplets with $D_{\text{wet}} \sim 2 \text{ mm}$, or a surface:volume ratio of 3000 m^{-1} . Values of σ obtained in macroscopic solutions have also been used in cloud parcel models (e.g., Ervens et al., 2005; Vanhanen et al., 2008), with results indicating an increase in cloud droplet concentrations of $\sim 10\%$ relative to those assuming $\sigma_{\text{H}_2\text{O}}$. However, it is not clear whether these macroscopic observations are germane to any surface tension reduction in $\sim 1 \mu\text{m}$ droplets, in which the surface:volume ratio is greater than 10^6 m^{-1} (Seidl and Hanel, 1983). This is because the amount of solute adsorbed at the interface is negligible relative to the amount in the bulk phase in macroscopic solutions, but becomes significant at higher surface:volume ratios characteristic of most real atmospheric particles. Recently, many studies have attempted to account for this by

High-RH hygroscopicity

C. R. Ruehl et al.

Title Page

Abstract

Introduction

Conclusions

References

Tables

Figures

◀

▶

◀

▶

Back

Close

Full Screen / Esc

Printer-friendly Version

Interactive Discussion



**High-RH
hygroscopicity**

C. R. Ruehl et al.

Title Page

Abstract

Introduction

Conclusions

References

Tables

Figures

◀

▶

◀

▶

Back

Close

Full Screen / Esc

Printer-friendly Version

Interactive Discussion



explicitly modeling the adsorption of solute to the droplet-air interface and the resulting depletion of solute in the droplet bulk phase. When this partitioning is taken into account, if insufficient solute is available to completely cover the interface, surface tension is reduced to a much lesser extent than in a macroscopic solution (Li et al., 1998; Sorjamaa et al., 2004; Topping et al., 2007), and/or depletion of solute in the bulk droplet increases droplet water activity (Sorjamaa and Laaksonen, 2006), in both cases resulting in a modeled cloud droplet concentration much closer to that obtained using $\sigma_{\text{H}_2\text{O}}$ (Kokkola et al., 2006). Partitioning strongly limits the increase in hygroscopicity due to solute surface activity relative to calculations that do not include it explicitly. Still, some authors have argued that the CCN activity of organic material can only be accurately predicted if σ is reduced to values similar to those observed in macroscopic solutions (Dinar et al., 2006; Asa-Awuku et al., 2008; Broekhuizen et al., 2004), although prediction of the CCN activity of known surface-active compounds in some studies has not required any reduction in σ (Abbatt et al., 2005; Sorjamaa et al., 2004). Also, recent work on organic aerosol particles produced from ozonolysis of α -pinene has suggested that only minor reductions in σ at activation are required to be consistent with hygroscopicity measured up to RH=99.6% (Wex et al., 2009).

In addition to surface tension reduction and partitioning, another property of many surface active compounds is the tendency to form micelles (or more generally, aggregates) above a certain concentration (the critical micelle concentration, C_{CMC}). C_{CMC} can be determined in macroscopic solutions by slowly adding a surface-active compound; at the C_{CMC} , the activity coefficient of that compound in solution, which can be conceptualized as the fraction of “free” (i.e., not in a micelle) molecules in solution, will decrease sharply, and other solution properties related to micellization, such as turbidity, may begin to change. Tabazadeh (2005) used accepted C_{CMC} values for typical surface-active compounds in theoretical calculations to argue that micellization occurs in aerosol solution droplets containing surface-active compounds, which would lower their hygroscopicity both by limiting the amount of solute available to partition to the air-droplet interface and by raising the water activity in the droplet relative to a

similar droplet in which no micellization occurs. However, as with measurements of the surface tension of macroscopic solutions, it is not clear that C_{CMC} values determined in such solutions are relevant to micron-sized droplets, with curved interfaces and much higher surface:volume ratios. In macroscopic solutions, the surface:volume ratio is small enough that the amount of solute at the interface can be neglected, and the C_{CMC} can be conceptualized as the concentration where the rate at which “free” molecules are incorporated into micelles is equal to the rate at which they leave micelles (i.e., steady-state). However, in micron-sized droplets, the amount of solute at the interface might no longer be negligible, meaning that “free” surface active molecules can either partition to the interface or form micelles, and thus the C_{CMC} would reflect the rate of both these reversible processes. In addition, the fact that the surface is curved could increase the tendency of a “free” molecule to partition to the surface, relative to its tendency to form a micelle.

The purpose of this study is to measure the hygroscopicity of aerosol particles of known composition at high RH. We use droplets with $D_{\text{wet}} \sim 1 \mu\text{m}$ for two reasons: first, as discussed above, such droplets are most sensitive to the Kelvin effect; and second, most cloud droplets are approximately this size in the early stages of cloud formation. We address three general questions related to high-RH hygroscopicity. First, how well can aerosol hygroscopicity be represented with a single parameter, as has been done in numerous recent studies (e.g., Petters and Kreidenweis, 2007; Hudson and Da, 1996; Wex et al., 2007), for relatively well-studied compounds at high values of RH (99.2 to 99.9%)? Second, to what extent does hygroscopicity determined for droplet sizes $\sim 1 \mu\text{m}$ differ from predictions based on properties of macroscopic solutions with much lower surface:volume ratios? And finally, if the hygroscopicity of individual compounds does vary within the range of experimental conditions, which processes might be responsible?

**High-RH
hygroscopicity**

C. R. Ruehl et al.

Title Page

Abstract

Introduction

Conclusions

References

Tables

Figures

◀

▶

◀

▶

Back

Close

Full Screen / Esc

Printer-friendly Version

Interactive Discussion



2 Theory

2.1 Parametrization of aerosol hygroscopicity

At elevated RH, atmospheric particles typically exist as solution droplets. Through condensation or evaporation of water, these droplets either grow or shrink until they reach equilibrium with ambient RH. In general, the more hygroscopic a particle, the more water it will absorb at a given RH. Although hygroscopicity is influenced by several physiochemical characteristics (e.g. molar volume, aqueous solution activity), it has been represented for both ambient and lab-generated particles by a single parameter based on Eq. (1), defined similarly but not identically in several studies (e.g., Fitzgerald et al., 1982; Hudson and Da, 1996; Wex et al., 2007; Petters and Kreidenweis, 2007). Because hygroscopicity is more sensitive to the Raoult term than the Kelvin term for all but the smallest particles at the highest RH (Fig. 1), most proposed parametrizations are defined through their effect on the water activity (a_w). To facilitate comparison with other studies, we use the commonly-used κ formulation of Petters and Kreidenweis (2007), in which κ relates a_w to the ratio of the volume of water to volume of solute in the droplet:

$$\kappa = \frac{V_w}{V_s} \left(\frac{1}{a_w} - 1 \right) \quad (3)$$

In this formulation, κ ranges from 0 for an insoluble but wettable substance to a maximum of approximately 1.3 for sodium chloride. Trends in hygroscopicity with RH, which are emphasized in this study, should be similar no matter which parametrization of the Raoult term is used.

Hygroscopicity can be represented by a single parameter, either with (e.g., Wex et al., 2007), or without (e.g., Duplissy et al., 2008) explicitly taking potential σ changes into account. If σ is assumed, then the hygroscopicity parameter incorporates any solute influence on the Kelvin effect as well as the Raoult effect. As discussed above, it is well known that particulate matter can significantly reduce σ of macroscopic aqueous

Title Page

Abstract

Introduction

Conclusions

References

Tables

Figures

◀

▶

◀

▶

Back

Close

Full Screen / Esc

Printer-friendly Version

Interactive Discussion



High-RH hygroscopicity

C. R. Ruehl et al.

Title Page

Abstract

Introduction

Conclusions

References

Tables

Figures

◀

▶

◀

▶

Back

Close

Full Screen / Esc

Printer-friendly Version

Interactive Discussion



solutions (by up to ~50%), but it remains unclear to what extent σ can be reduced in droplets with $D_{\text{wet}} \sim 1 \mu\text{m}$. We wish to incorporate all factors influencing hygroscopicity into a single parameter, without introducing additional parameters such as those in the Szyszkowski equation (Szyszkowski, 1908) which is typically used to express σ as a function of solute concentration. Our approach is therefore to assume $\sigma = \sigma_{\text{H}_2\text{O}}$, and we therefore rewrite Eq. (1) using the definition of κ (Eq. 3):

$$\text{RH} = \frac{D_{\text{wet}}^3 - D_{\text{dry}}^3}{D_{\text{wet}}^3 - D_{\text{dry}}^3 (1 - \kappa)} \exp\left(\frac{4\sigma_{\text{H}_2\text{O}}}{RT\overline{V}_w D_{\text{wet}}}\right) \quad (4)$$

If the actual surface tension of the droplet is lower, we will measure a larger κ because its D_{wet} , and therefore \overline{V}_w , will be larger than that of an equivalent droplet with $\sigma = \sigma_{\text{H}_2\text{O}}$.

As can be seen in Eq. (4), κ is a parametrization of the Raoult term in Eq. (1), and therefore includes an assumed surface tension. For these reasons, κ is a more useful indicator of the Raoult effect than the Kelvin effect. To examine the Kelvin effect, which goes as D_{wet}^{-1} , we instead use a parametrization of the Kelvin term. This requires that we make an assumption regarding the Raoult term. If we assume an ideal solution, the water activity is equal to the exponential of the solute mole fraction:

$$a_{w,\text{ideal}} = \exp\left(-\frac{\nu_s n_s}{n_w}\right) \quad (5)$$

where ν_s is the van't Hoff factor (the moles of soluble species per mole solute), and n_s and n_w are the moles of solute and water, respectively, in the droplet. We then define a length scale (Lewis, 2008):

$$\delta = \frac{4\sigma\overline{V}_w}{RT} \quad (6)$$

and substitute into the Köhler equation:

$$\text{RH} = \exp\left(-\frac{\nu_s n_s}{n_w}\right) \exp\left(\frac{\delta}{D_{\text{wet}}}\right) \quad (7)$$

For a droplet at 25°C with the surface tension of pure water, $\delta=2.1$ nm, and because $\delta \propto \sigma$, as hygroscopicity increases, δ decreases. For most non-ideal solutions, a_w is greater than $a_{w,\text{ideal}}$, and therefore in general δ will increase as the solution droplet deviates further from ideality.

5 2.2 Influence of the Raoult effect on κ

The presence of solute in a droplet increases its hygroscopicity by reducing the fraction of solvent (water) in the droplet, resulting in a reduced water activity (a_w). As stated previously, this is known as the Raoult effect on aerosol hygroscopicity, and is important over a wide range of RH and D_{wet} . a_w depends on the chemical identity of the solute, as well as the molar ratio of solute to water in the droplet:

$$a_w = \exp\left(-\frac{\phi v_s n_s}{n_w}\right) \quad (8)$$

which differs from $a_{w,\text{ideal}}$ (Eq. 5) only in that the term in the exponential is multiplied by ϕ , the molal osmotic coefficient. n_s depends on the size of the dry particle:

$$n_s = \frac{\pi D_{\text{dry}}^3}{6\bar{V}_s} \quad (9)$$

15 where D_{dry} is the diameter of the dry particle and \bar{V}_s is the molar volume of the solute, and n_w depends on D_{wet} after the volume of solute has been subtracted:

$$n_w = \frac{\pi (D_{\text{wet}}^3 - D_{\text{dry}}^3)}{6\bar{V}_s} \quad (10)$$

Given D_{dry} and \bar{V}_s , Eqs. (8, 9, and 10) can be used with Eq. (1) to solve for D_{wet} as a function of RH, and Eq. (4) is used to solve for κ corresponding to each D_{wet} .

Title Page

Abstract

Introduction

Conclusions

References

Tables

Figures

◀

▶

◀

▶

Back

Close

Full Screen / Esc

Printer-friendly Version

Interactive Discussion



High-RH hygroscopicity

C. R. Ruehl et al.

Title Page

Abstract

Introduction

Conclusions

References

Tables

Figures

◀

▶

◀

▶

Back

Close

Full Screen / Esc

Printer-friendly Version

Interactive Discussion



For most solutes, ϕ as a function of $\frac{n_s}{n_w}$ is well known based on measurements of the water activity of macroscopic solutions, even at the upper end of the range of a_w that is the focus of this study. For sodium chloride, ammonium sulfate, and malonic acid, we used the E-AIM water activity model to determine ϕ (Clegg et al., 1998, 2001), and use Eqs. (3 and 8) to calculate κ as a function of RH (assuming a surface tension of pure water). This model is based on experimental water activities measured in macroscopic solutions, and we compare our experimental results to it to determine how valid it may be for microscopic droplets. For sucrose and glucose, we also compared our data to predictions based on macroscopic experimental values (Clegg et al., 2001; Stokes and Robinson, 1966), which indicates that $\phi > 1$ for these sugars. For all compounds, our experimental data is compared to that predicted for an ideal solution ($\phi = 1$).

To examine the Raoult effect, we examine how, if at all, κ for seven compounds varies with RH between 99 and 100%. Combining Eqs. (3 and 8), it can be shown that, if $\text{RH} \approx 100\%$,

$$\kappa \simeq v_s \phi \bar{V}_w / \bar{V}_s \quad (11)$$

For an ideal, non-surface active solute, κ is essentially constant throughout the range of RH examined in this study. For non-ideal, non-surface active solutes, κ is proportional to ϕ . For surface-active solutes, σ is reduced, which in turn raises κ an amount that increases with increasing RH. While the increase in κ is sensitive to RH, it is reasonably insensitive to D_{dry} (Fig. 2a). This is a desirable quality in any hygroscopicity parameter, and is due to the dependence of κ on the volumetric ratio of water to solute in a droplet. Not all dependence on D_{dry} is removed, however, unless the surface tension of the droplet equals the assumed surface tension used in Eq. (4). Note that the sensitivity of κ to D_{dry} is much greater if one looks for a trend in κ with D_{wet} (Fig. 2b).

2.3 Influence of the Kelvin effect on δ

As discussed previously, we parametrize the Kelvin term in the Köhler equation to examine trends in hygroscopicity with droplet diameter (D_{wet}) using the length scale

High-RH hygroscopicity

C. R. Ruehl et al.

δ as defined in Eq. (7), which is proportional to surface tension (σ). This requires a value of ϕ , which we assume is a function of RH and obtain from the linear regression of κ onto RH. This, along with the fact that δ is a parametrization of the Kelvin term in the Köhler equation, are the two main distinctions between δ and κ . If the surface tension of a solution droplet is lower than that of pure water, but the depletion of solute in the bulk phase is negligible, the observed value of δ will be lower than that of an ideal solution droplet with $\sigma = \sigma_{\text{H}_2\text{O}}$ (Fig. 2c). δ is sensitive to the assumed value of ϕ , however, and therefore we derive δ using several constant values of ϕ , as well as the linear relationship between ϕ and RH derived from the regression of κ onto RH. These are used to probe the sensitivity of any trend in δ with D_{wet} to the assumption of ϕ .

If a solute in a solution droplet is surface-active, it will preferentially partition to the droplet-air interface and reduce the surface tension of the interface below the value for pure water. This reduces the Kelvin term in the Köhler equation and consequently increases hygroscopicity. The surface:volume ratio and the curvature of the droplet depends on the droplet diameter (D_{wet}), and we can therefore evaluate the Kelvin effect by examining the dependence of δ on D_{wet} for sodium dodecyl sulfate (SDS), a model surface-active compound. σ of aqueous solutions of such compounds typically varies with bulk concentration according to the Szyszkowski equation (Chang and Franses, 1995; Szyszkowski, 1908):

$$\sigma = \sigma_{\text{H}_2\text{O}} - \nu_s RT \Gamma_m \ln(1 + K_L C_{\text{bulk}}) \quad (12)$$

where Γ_m is the maximum surface concentration and K_L is the equilibrium partitioning coefficient, two parameters that are fit to surface tension measurements of macroscopic solutions. For SDS, the parameters are typically set to $\Gamma_m = 1.0 \times 10^{-5} \text{ mol m}^{-2}$ and $K_L = 1.1 \times 10^{-1} \text{ m}^3 \text{ mol}^{-1}$ (Chang et al., 1992), and C_{bulk} is not allowed to increase above the critical micelle concentration ($C_{\text{CMC}} = 8.2 \text{ mol m}^{-3}$) which prevents σ from being lowered beyond a certain minimum (41 mJ m^{-2} if $\Gamma_m = 1.0 \times 10^{-5} \text{ mol m}^{-2}$). A more physical value of Γ_m is $6 \times 10^{-6} \text{ mol m}^{-2}$, as this corresponds to a more realistic cross-sectional area of 30 \AA^2 per molecule (Prosser and Franses, 2001). The range of SDS

Title Page

Abstract

Introduction

Conclusions

References

Tables

Figures

◀

▶

◀

▶

Back

Close

Full Screen / Esc

Printer-friendly Version

Interactive Discussion



concentrations observed in this study is 110 to 340 mol m⁻³, the entirety of which is more than 10 times greater than C_{CMC} , suggesting that for all SDS solution droplets, excess SDS will be present to reduce σ to whatever minimum value corresponds to a complete (monolayer) coverage of the interface by SDS. We also took partitioning into account, by assuming that the solute was distributed between the bulk solution and the surface (Sorjamaa et al., 2004; Li et al., 1998):

$$n_s^{\text{tot}} = n_s^{\text{bulk}} + n_s^{\text{surf}} \quad (13)$$

Although in more dilute solutions an isotherm might be used to relate n_s^{bulk} and n_s^{surf} , under the relatively large SDS concentrations observed here (110 to 340 mol m⁻³), we assume that the maximum surface concentration is achieved, and therefore:

$$n_s^{\text{surf}} = \pi D_{\text{wet}}^2 \Gamma_m \quad (14)$$

This model of the SDS solution droplet with a complete coating of solute at the droplet-air interface is similar to the “inverted micelle” model of solution droplets with organic solutes that has been previously described (Gill et al., 1983; Ellison et al., 1999), and for which some observational evidence has been obtained (e.g., Husar and Shu, 1975; Tervahattu et al., 2002; Russell et al., 2002). However, this blurs the distinction between soluble (e.g., SDS) and insoluble (e.g., fatty acids) surfactants. For a soluble surfactant, the excess surface concentration might not all reside at the interface, but could be a part of a concentration gradient between the bulk and surface phases. To the extent that partitioning does deplete solute from the bulk phase, hygroscopicity will decrease and δ will therefore be greater. Furthermore, like σ this effect goes as D_{wet}^{-1} , and therefore δ is a convenient metric for both the effect of σ reduction and partitioning.

2.4 Specific questions addressed by this study

We compare hygroscopicity (our experimental values of κ and δ) to values calculated under different assumptions regarding the terms a_w (i.e., the Raoult effect) and σ (i.e.,

[Title Page](#)
[Abstract](#)
[Introduction](#)
[Conclusions](#)
[References](#)
[Tables](#)
[Figures](#)
[Back](#)
[Close](#)
[Full Screen / Esc](#)
[Printer-friendly Version](#)
[Interactive Discussion](#)


the Kelvin effect) in Eq. (1). We use observations of aerosol hygroscopicity to answer the following specific questions:

1. How, if at all, does κ vary with RH (the Raoult effect)?
2. How, if at all, does δ vary with D_{wet} (the Kelvin effect)?
- 5 3. For our model surface-active compound (SDS), does partitioning of solute to the droplet-air interface and the resulting depletion in the bulk droplet need to be taken into account to accurately predict hygroscopic growth?
4. And finally, do we see evidence that micellization of SDS limits its hygroscopicity?

3 Experimental

10 Particles of known composition were generated by atomizing aqueous solutions with a high-pressure nitrogen jet. After atomization, particles flowed through two diffusion driers, which lowered the RH of the flow to below 10%. After drying, particles entered a differential mobility analyzer (DMA, manufactured by TSI), which selected particles of a certain electrical mobility. While this quasi-monodisperse population was primarily
15 made up of singly-charged particles with diameters (D_{dry}) between 0.2 and 0.5 μm , it always included some larger, multiply-charged particles of equal mobility (and consequently a predictable D_{dry} following from the D_{dry} of the singly-charged particles). The sheath and sample flow rate in the DMA were 2 and 0.2 L min^{-1} , respectively. The quasi-monodisperse flow was split, with half going to a condensation nucleus counter and half going to a continuous-flow thermal gradient column (CFTGC). A dynamic shape correction factor (χ) of 1.08 was used for NaCl aerosol, 1.04 for ammonium sulfate (AS) aerosol, and no shape correction was made ($\chi=1$) for any of the organic aerosol tested (Zelenyuk et al., 2006; Krämer et al., 2000).

25 Flow in the CFTGC proceeds through 1 m of stainless steel tubing with an ID of 0.022 m. Temperature is controlled at four locations along the tube with high-precision

Title Page

Abstract

Introduction

Conclusions

References

Tables

Figures

◀

▶

◀

▶

Back

Close

Full Screen / Esc

Printer-friendly Version

Interactive Discussion



**High-RH
hygroscopicity**

C. R. Ruehl et al.

Title Page

Abstract

Introduction

Conclusions

References

Tables

Figures

I◀

▶I

◀

▶

Back

Close

Full Screen / Esc

Printer-friendly Version

Interactive Discussion



thermistors and thermo-electric coolers. The inside wall of the tubing is coated with filter paper, which is saturated with water before use. In previous experiments, the CFTGC has been operated in “CCN” mode, in which a positive temperature gradient (ΔT) was imposed in the direction of the flow (Ruehl et al., 2008). Water vapor diffuses more quickly from the inner wall to the centerline than does the bulk gas (due to its lower molecular mass), causing a supersaturation ($RH > 100\%$) along the centerline. This technique of producing a supersaturation was described in Roberts and Nenes (2005). In the experiments of this study, the CFTGC was operated in “high-RH” mode: a negative ΔT in the direction of flow was applied, and water vapor diffused more rapidly from the centerline to the inner walls, lowering the RH along the centerline below unity, to somewhere in the range of 99.2 to 99.9% (depending on ΔT). The overall flow rate in the column was 0.94 L min^{-1} , of which 0.1 L min^{-1} was the quasi-monodisperse flow along the centerline, and the remainder was a humidified, particle-free sheath flow.

Before exiting the CFTGC, the diameter and velocity of droplets along the centerline was measured with a phase Doppler interferometer (PDI) manufactured by Artium Technologies, Inc. (Bachalo, 1980; Bachalo and Houser, 1984). Diameters were binned at $0.1 \mu\text{m}$ intervals. To get a sense of the precision of these measurements, we measured D_{wet} spectra at $\Delta T = 1 \text{ K}$ for droplets formed on dry NaCl particles. The mobility diameter of the NaCl particles was increased from 100 nm to 400 nm at 10 nm intervals (Fig. 3). Larger droplets formed on larger, multiply-charged particles were resolved in most spectra. A bimodal (both normally-distributed) fit was found for each spectra, and the smaller D_{wet} mode (which was always the more numerous) was assumed to be the singly-charged mode. The standard deviation of this mode ranged from 0.10 to $0.42 \mu\text{m}$, or from 7 to 22% of the mean. Replicate measurements of D_{wet} standard deviation were made at several D_{dry} , and ranged from 0.03 to $0.30 \mu\text{m}$ (3 to 15% of the mean). However, when restricted to $D_{\text{wet}} < 2.0 \mu\text{m}$, which includes all droplets in this study except those formed on the largest NaCl and AS particles, standard deviations of replicate measurements ranged from 0.03 to $0.13 \mu\text{m}$ (3 to 9% of the mean).

**High-RH
hygroscopicity**

C. R. Ruehl et al.

Title Page

Abstract

Introduction

Conclusions

References

Tables

Figures

◀

▶

◀

▶

Back

Close

Full Screen / Esc

Printer-friendly Version

Interactive Discussion



RH in the CFTGC was calibrated with NaCl particles, which required an assumption of κ . Based on the E-AIM model (Clegg et al., 1998, 2001), we assumed NaCl κ increased slightly over the relevant RH range, from 1.24 to 1.27, and then used Eq. 4 to relate RH to D_{wet} of NaCl solution droplets at a given ΔT . We found a linear relationship between RH and ΔT , but saw slight variation in absolute RH ($\sim 0.05\%$) at the same ΔT on different days (Fig. 4). Therefore instead of utilizing the linear regression of RH onto ΔT , for all compounds besides NaCl we transformed D_{wet} into κ using the NaCl-calibrated RH for the individual day of the measurements. It should be mentioned that RH is very sensitive to T , such that an increase in T of only 0.015 K would result in a decrease in RH of 0.1%. This calibration therefore suggests that the temperature in the view volume was stable to within ~ 0.01 K, which is approximately the precision of the thermistors.

4 Results and discussion

4.1 Overall results

As expected, the high-RH hygroscopicity of both inorganic compounds was greater than that of any of the five organic compounds (Table 1, Fig. 5). NaCl was the most hygroscopic compound studied ($\kappa = 1.27 \pm 0.11$), followed by ammonium sulfate (AS $\kappa = 0.572 \pm 0.074$). Because NaCl was used as the reference compound, the average value of NaCl κ was set to match macroscopic observations at high RH. The observed standard deviation of NaCl κ (0.11) was mostly due to experimental uncertainty, arising from variation in the RH within the view volume, and to a lesser extent uncertainty in the value of D_{wet} measured by the PDI. (As mentioned before, a change in RH of 0.1% would result from a temperature fluctuation of only 0.015 K.) Average AS κ was 21% lower than the ideal value (0.72) but in agreement with the value predicted from macroscopic observations (Timmermans, 1960). If the nonideality of AS is incorporated into the van't Hoff factor, this is equivalent to an average value of $\nu = 2.4$, although

as discussed below this value increases over the RH range studied here.

Although not found in atmospheric particles (Facchini et al., 2001), sodium dodecyl sulfate (SDS) is a commonly studied surfactant, and as such it was used as a model surface-active compound. The high-RH hygroscopicity of SDS was measured for 53 different combinations of D_{dry} and RH, yielding $\kappa=0.134\pm0.029$. This variability was similar to that observed for inorganic compounds, and at least partly due to experimental uncertainties. If SDS formed an ideal aqueous solution, κ as predicted by Eq. (11) would be 0.147; therefore assumption of ideality results in only a 9% relative error. In macroscopic solutions, however, SDS does not behave ideally. At infinite dilution, $\phi=0.75$ (Widera et al., 2003), which in Eq. (11) yields $\kappa=0.110$, or 18% below the mean high-RH value. Also, again in macroscopic solutions, ϕ drops sharply to 0.12 as the critical micelle concentration (C_{CMC} , 8.2 mol m^{-3}) is approached, and remains at 0.12 for all $[\text{SDS}] \geq C_{\text{CMC}}$ (Widera et al., 2003). This range includes all solution droplets measured in this study, and thus the high hygroscopicity of SDS suggests that surface tension reduction and/or a lack of micellization in micron-sized solution droplets enhances SDS aerosol hygroscopicity at high RH.

Data for the remaining compounds was more limited. As with the inorganic compounds, the relative hygroscopicity of the organic compounds was as predicted from their molar volumes and assuming an ideal solution (Fig. 5, Table 1). Malonic acid was the most hygroscopic organic compound ($\kappa=0.29$), followed by adipic acid (0.19), glucose (0.17), sodium dodecyl sulfate (0.13), and sucrose (0.11). Malonic acid κ was only slightly above the theoretical value assuming ideality and no dissociation. Glucose hygroscopicity was also slightly greater than that predicted for an ideal solution. In contrast, sucrose hygroscopicity was 25 to 50% greater than that predicted assuming ideality. Adipic acid hygroscopicity was relatively high, especially in light of negligible adipic acid hygroscopicity that has been observed in several studies. This could be due to the relatively large size ($D_{\text{dry}} \geq 250 \text{ nm}$) of adipic acid particles examined, which are not subject to the deliquescence barrier to hygroscopic growth affecting smaller ($D_{\text{dry}} < 150 \text{ nm}$) particles (Hings et al., 2008).

**High-RH
hygroscopicity**

C. R. Ruehl et al.

Title Page

Abstract

Introduction

Conclusions

References

Tables

Figures

◀

▶

◀

▶

Back

Close

Full Screen / Esc

Printer-friendly Version

Interactive Discussion



4.2 Hygroscopicity variation with RH

4.2.1 Inorganic compounds

Because NaCl was used as the reference substance (Fig. 4), theoretical variation of κ with RH was determined by experimental NaCl water activity data, as incorporated into the E-AIM water activity model, and increased from 1.24 at RH=99.2% to 1.27 at RH=99.9%, a small variation relative to that due to experimental uncertainty (Fig. 6a). The agreement between the calibrated observations and the E-AIM predictions reflects the linearity of the RH vs. ΔT calibration in the CF-TGC.

κ of ammonium sulfate increased slightly as RH increased from 99 to 100%, as predicted using macroscopic water activity measurements (represented by E-AIM, see Fig. 6b). Although this trend had only mild statistical significance ($p=0.068$, see Table 1), the excellent match between the observations and the E-AIM predictions suggests that micron-sized AS solution droplets can be described by macroscopic data. If this nonideality were to be incorporated into the van't Hoff factor, it would increase from $\nu=2.2$ to 2.5 as RH increases from 99.2 to 99.9%, suggesting that a value larger than 2.5 should be used in calculations involving activation of AS particles under supersaturated conditions.

4.2.2 SDS

In macroscopic aqueous solutions, the ability of SDS to lower water activity (a_w) is strongly limited by its tendency to form micelles, and therefore its hygroscopicity might be expected to increase with increasing RH, as greater dilution would reduce the proportion of SDS found in micelles. However, as with NaCl, the hygroscopicity of SDS did not vary with RH (Fig. 7a). This indicates either that SDS ϕ is relatively constant at high RH, or that variation in ϕ is roughly canceled out by SDS surface activity in terms of its influence on hygroscopicity. To further investigate this lack of variation, we make several assumptions regarding the water activity of SDS solution droplets, and

Title Page

Abstract

Introduction

Conclusions

References

Tables

Figures

◀

▶

◀

▶

Back

Close

Full Screen / Esc

Printer-friendly Version

Interactive Discussion



compare the predicted variation in SDS κ with RH to observations.

Our first two assumptions are that SDS behaves ideally ($\phi_{\text{SDS}}=1$), and that its activity matched the observed average value of κ ($\phi_{\text{SDS}} = \frac{\kappa_{\text{obs}}}{\kappa_{\text{ideal}}}=0.91$). In both cases, the surface tension of the droplet is assumed to be equal to that of pure water. The resulting values of SDS κ are constant with RH (Fig. 8a) both because ϕ is constant and $\sigma=72.8 \text{ mJ m}^{-2}$ (the assumed value in the κ formulation, see Eq. 4). Additionally, the theoretical κ values are roughly consistent with the observed values. However, if it is assumed that $\phi=0.12$, as it does in macroscopic SDS solutions of the same concentration, κ is much smaller than in our observations (Fig. 8a). This is true even if σ is assumed to be zero, because the increase in hygroscopicity resulting from this assumption is overwhelmed by the water activity increase associated with $\phi=0.12$ (Fig. 8a). Also, at this RH, even if a full monolayer formed at the droplet surface, sufficient SDS would remain to exceed the CMC in the bulk phase. We therefore conclude that micellization in micron-sized SDS solution droplets does not increase a_w at RH from 99 to 100% in a manner analogous to macroscopic solutions, and thus that C_{CMC} values obtained from measurements of such solutions may not be appropriate for calculations involving aerosol particles of typical atmospheric sizes (e.g., Tabazadeh, 2005).

4.2.3 Other organic compounds

The hygroscopicity of remaining compounds, all organic, increased with RH, with the exception of sucrose. These trends were most significant for malonic acid ($p<0.01$) and sucrose ($p<0.03$, Table 1). Like AS, the increase of malonic acid κ with RH was consistent with the E-AIM activity coefficient model (Fig. 9a), and values of $\kappa>\kappa_{\text{ideal}}$ around RH=99.8% are likely due to dissociation (κ was calculated assuming no dissociation).

Glucose hygroscopicity increased slightly with RH (Fig. 9b). Unlike the inorganic compounds, for glucose $\phi>1$ in aqueous solutions (e.g., Matubayasi and Nishiyama, 2006), from which $\kappa>\kappa_{\text{ideal}}$ follows. At the high RH observed in this study, glucose

Title Page

Abstract

Introduction

Conclusions

References

Tables

Figures

◀

▶

◀

▶

Back

Close

Full Screen / Esc

Printer-friendly Version

Interactive Discussion



High-RH hygroscopicity

C. R. Ruehl et al.

Title Page

Abstract

Introduction

Conclusions

References

Tables

Figures

◀

▶

◀

▶

Back

Close

Full Screen / Esc

Printer-friendly Version

Interactive Discussion



concentration was between 0.11 to 0.45 mol kg^{-1} , which in macroscopic solutions corresponds to an increase in ϕ of $<2\%$ (Stokes and Robinson, 1966), and thus this effect would have to be enhanced in micron-sized droplets to account for the observations.

Sucrose was the only compound studied in which κ decreased with RH (Fig. 9c), although for all RH, $\kappa > \kappa_{\text{ideal}}$. Like glucose, the osmotic coefficient of macroscopic sucrose solutions is greater than one, although sucrose deviates further from ideality (which is consistent with our observations). At the maximum sucrose concentration observed (0.53 mol kg^{-1}), $\phi = 1.044$ in macroscopic solutions (Clegg et al., 2001), again suggesting that this effect is enhanced in micron-sized droplets relative to macroscopic solutions. The ratio of glucose κ to sucrose κ increases towards 1.8 (the ratio of their molar volumes, as assumed for ideal solutions) as $\text{RH} \rightarrow 100\%$. The greater non-ideality of sucrose relative to glucose is already apparent at $\text{RH} \sim 99.5\%$.

An increase in adipic acid κ with RH (Fig. 9d) could also at least partly be caused by its low solubility of 25 kg m^{-3} (Saxena and Hildemann, 1996). Again assuming $\phi = 1$, this solubility limit corresponds to an RH of $\sim 99.7\%$. Adipic acid κ does decrease below this limit, although it is consistently larger than predicted without accounting for dissociation (or Kelvin effects).

4.3 Hygroscopicity variation with D_{wet}

4.3.1 Comparison of κ and δ as a hygroscopicity parameter vs. D_{wet}

We first compared κ and δ as a parameter for trends in hygroscopicity with D_{wet} to see if there was any justification for a second parameter. Calculation of δ requires assumption of ϕ (i.e., the Raoult effect), and we allow ϕ to vary with RH according to the linear regression of κ onto RH (red lines in Figs. 6, 7a, and 9). We therefore expect δ to be a more conservative metric of Kelvin effects, because it attempts to account for the Raoult effect. This can be seen by comparing the ρ values for these parameters (Table 2), which are generally higher (less significant) for δ . δ for only two compounds (SDS and malonic acid) varied significantly ($p < 0.05$) with D_{wet} , while variation of κ with

**High-RH
hygroscopicity**C. R. Ruehl et al.

[Title Page](#)[Abstract](#)[Introduction](#)[Conclusions](#)[References](#)[Tables](#)[Figures](#)[◀](#)[▶](#)[◀](#)[▶](#)[Back](#)[Close](#)[Full Screen / Esc](#)[Printer-friendly Version](#)[Interactive Discussion](#)

D_{wet} was significant for two additional compounds (glucose and adipic acid). Figure 7b and c show the trend in SDS hygroscopicity with D_{wet} using κ and δ , respectively. The trends are in opposite direction because hygroscopicity decreases with δ , but the significance (Table 2) and the correlation are similar. Based on the results from all compounds, we conclude that a parameterization of the Kelvin term that accounts for nonideality ($\phi \neq 1$) such as δ is a more conservative and in that sense a useful metric of Kelvin effects in micron-sized droplets.

4.3.2 Inorganic compounds

Neither NaCl nor AS δ varied with D_{wet} (Fig. 10), as expected because these salts are not known to be surface-active. The finding that non-ideal behavior of AS, as opposed to surface activity, causes variation in high-RH hygroscopicity is consistent with LACIS measurements (Wex et al., 2005).

4.3.3 Sodium Dodecyl Sulfate (SDS)

It is well-known that SDS reduces the surface tension (σ) of macroscopic aqueous solutions, and consequently one might expect SDS δ to be lower than that of NaCl and AS. SDS hygroscopicity did vary strongly with D_{wet} (Fig. 7b and c), although it is not immediately clear why its surface activity causes its hygroscopicity to increase with increasing D_{wet} , as a given reduction in surface tension would be expected to cause a decrease in δ_{SDS} which does not vary with D_{wet} . Next, we make a series of assumptions regarding SDS surface activity, and discuss the theoretical variation in κ with RH and δ with D_{wet} resulting from these assumptions.

As can be seen in Eq. (6), δ is proportional to surface tension (σ). If SDS solution droplets behave ideally, with a surface tension of pure water, δ is equal to 2.1 nm, and $\delta=0$ if the Kelvin effect is completely neglected (Fig. 11a). Taking surface partitioning into account has the opposite effect: formation of a monolayer (surface excess concentration, Γ , of $6 \mu\text{mol m}^{-2}$) causes δ to increase to 3.6 nm (Fig. 11a). With a soluble

surfactant such as SDS, it is likely that the surface excess concentration exists in a finite volume bounded on the outside by the droplet-air interface, and not only at the interface, and thus concentrations greater than a monolayer equivalent are physically reasonable. Note that like σ , the influence of Γ on hygroscopicity goes as D_{wet}^{-1} , and therefore δ is constant with D_{wet} .

Transformation of observed D_{wet} into δ requires an assumption of ϕ for the solution droplets. As with all other compounds, for SDS we assumed that solution activity varies with RH according to the linear regression of κ onto RH (for SDS, ϕ was relatively constant, roughly 0.9). To test the sensitivity of the trend in δ with D_{wet} to this assumption, we repeat the calculations assuming $\phi=0.75$ (Fig. 11b). This causes a slight downward shift in all δ , but the trend in δ with D_{wet} is not fundamentally altered.

It can be seen in Fig. 11a that lowering surface tension and accounting for surface partitioning have opposite effects on SDS hygroscopicity (parametrized as δ). When both are taken into account, they tend to cancel each other out, and if they are roughly in balance, no trend in hygroscopicity with RH would be predicted (Fig. 8b). The lack of a trend in SDS κ with RH therefore suggests that surface tension lowering is roughly canceled out by surface partitioning in terms of its effect on SDS hygroscopicity.

As indicated above, we have not been able to model the observed increase in SDS hygroscopicity (decrease in δ_{SDS}) with D_{wet} assuming constant values of ϕ , σ , and Γ . This suggests that at least one of these parameters varies with D_{wet} . Because κ is roughly proportional to ϕ , and the highest observed values of κ_{SDS} are roughly 2 times greater than the lowest, the range of observed SDS hygroscopicity could correspond to an increase in ϕ from 0.5 to 1. This could result from micellization in smaller droplets, although not to the extent seen in macroscopic solutions. However, ϕ is typically thought to vary with concentration, and thus a trend in κ_{SDS} with RH would be expected if ϕ is not constant. It is therefore unlikely that the trend in δ is the result of micellization.

Figure 8b demonstrates that if both σ and Γ are allowed to vary with D_{wet} , they can do so in a way that their influences on the κ vs. RH trend cancel out. We found that

High-RH hygroscopicity

C. R. Ruehl et al.

[Title Page](#)[Abstract](#)[Introduction](#)[Conclusions](#)[References](#)[Tables](#)[Figures](#)[◀](#)[▶](#)[◀](#)[▶](#)[Back](#)[Close](#)[Full Screen / Esc](#)[Printer-friendly Version](#)[Interactive Discussion](#)

**High-RH
hygroscopicity**

C. R. Ruehl et al.

Title Page

Abstract

Introduction

Conclusions

References

Tables

Figures

◀

▶

◀

▶

Back

Close

Full Screen / Esc

Printer-friendly Version

Interactive Discussion



the following assumptions fit the observations: At the low end of our measured D_{wet} ($0.8 \mu\text{m}$), we set Γ to $18 \mu\text{mol m}^{-2}$, and decreased Γ linearly with D_{wet} until $\Gamma=0$ when $D_{\text{wet}}=1.8 \mu\text{m}$. We held σ constant at 30mJ m^{-2} . Under these assumptions, κ does not vary with RH (Fig. 12a), but δ would decrease with D_{wet} at roughly the observed rate (Fig. 12b). We emphasize that because two effects are opposing each other (surface tension reduction and partitioning), we cannot isolate either effect and thus these values can not be considered independent estimates. In other words, this model is an ad hoc fit to the data, and while we can conclude that SDS hygroscopicity increases with increasing D_{wet} , the mechanism responsible for this trend remains unclear.

As mentioned in the introduction, a value of Γ corresponding to the actual size of the SDS molecule is $6 \mu\text{mol m}^{-2}$ if a monolayer is present. Previous investigations have characterized two types of organic films at aqueous interfaces: “condensed” films formed by insoluble organic matter, which resides only at the aqueous-air interface, and “adsorbed” films formed by soluble organic matter. Because SDS is a soluble surfactant, its surface excess might occur both at the interface, but also as an increased dissolved concentration near the interface (i.e., a gradient from the interface to the bulk). In other words, if the surface excess concentration is $18 \mu\text{mol m}^{-2}$ but only $6 \mu\text{mol m}^{-2}$ can reside in a monolayer at the interface, then for every SDS molecule in the monolayer, there are two in solution near the interface in excess of the bulk solution concentration. This interpretation of the surface excess concentration is supported by measurements of evaporation rates from SDS solutions, which are similar to those of pure water. In contrast, a compressed film of insoluble surfactant can substantially reduce evaporation rates from aqueous solutions (Nakahara et al., 2008). However the same effect could result from any mechanism causing a decrease in SDS solution activity that is goes as D_{wet}^{-1} .

4.3.4 Other organic compounds

The hygroscopicity of all other organic compounds increased with size (i.e., δ decreased with D_{wet}), although none as strongly as SDS (Fig. 13). As with the variation of hygroscopicity with RH, this trend was strongest (Fig. 13a) and most significant ($p=0.014$, Table 2) for malonic acid, followed by sucrose. These results therefore provide evidence that both the Raoult and Kelvin effects influence the high-RH hygroscopicity of malonic acid and, to a lesser extent, sucrose. It is also possible that the Kelvin effect contributes to the hygroscopicity of both sugars. While glucose is known to slightly raise the surface tension of aqueous solutions, sucrose has the opposite effect (Matubayasi and Nishiyama, 2006), and this is consistent with sucrose δ being lower on average than glucose δ . The change in σ of macroscopic solutions caused by these sugars is slight relative to SDS, however, particularly at low concentrations. Furthermore, without independent knowledge of the osmolality of these droplets, the importance of the Kelvin effect on sugar hygroscopicity cannot be quantified. An increase in adipic acid hygroscopicity (represented by κ) with D_{wet} was not seen when δ was calculated taking the change in κ with RH into account (Fig. 13d, Table 2).

5 Conclusions

The hygroscopicity of particles of seven pure compounds was measured at RH ranging from 99.2 to 99.9%, and expressed as κ to examine the Raoult effect and as δ to examine the Kelvin effect. The observed hygroscopicities were broadly consistent with those predicted based on the chemical properties (molar volume, water activity) of the compounds. For the inorganic compounds (NaCl and ammonium sulfate), hygroscopicity was relatively constant with both RH and D_{wet} , and the small amount of variability could be explained using only variation in ϕ (i.e., the Raoult effect). In contrast, variability in hygroscopicity was greater for all five organic compounds, suggesting that for most compounds surface activity (both σ reduction and surface partitioning) in addition

Title Page

Abstract

Introduction

Conclusions

References

Tables

Figures

◀

▶

◀

▶

Back

Close

Full Screen / Esc

Printer-friendly Version

Interactive Discussion



**High-RH
hygroscopicity**

C. R. Ruehl et al.

to non-ideal behavior affects hygroscopicity (i.e., both the Kelvin and Raoult effects are important). Organic hygroscopicity generally increased with increasing D_{wet} , particularly so for the most surface active compound, sodium dodecyl sulfate (SDS). Although the mechanism remains unclear, κ_{SDS} increased by roughly a factor of two as D_{wet} increased from 1 to 2 μm . Therefore surface activity hinders hygroscopicity for a model soluble surfactant, likely due to surface partitioning which becomes less important as droplet size increases. Given reasonable assumptions of surface tension, the surface excess concentration of SDS in smaller droplets was greater than one monolayer thick, which is consistent with it being a soluble surfactant. SDS hygroscopicity was much higher than predicted assuming that micellization limits SDS activity to the extent observed in macroscopic solutions. These results therefore suggest that measurements of the surface-active properties of macroscopic aqueous solutions may not be appropriate at the much higher surface:volume ratios found in activating cloud droplets.

Acknowledgements. The authors would like to acknowledge funding from the NASA Radiation Sciences Program and the NSF Graduate Research Fellowship program.

References

- Abbatt, J. P. D., Broekhuizen, K., and Kumal, P. P.: Cloud condensation nucleus activity of internally mixed ammonium sulfate/organic acid aerosol particles, *Atmos. Environ.*, 39, 4767–4778, doi:10.1016/j.atmosenv.2005.04.029, 2005. 15600
- Abdul-Razzak, H. and Ghan, S. J.: Parameterization of the influence of organic surfactants on aerosol activation, *J. Geophys. Res.-Atmos.*, 109, 1–11, doi:10.1029/2003JD004043, 2004. 15599
- Asa-Awuku, A., Sullivan, A. P., Hennigan, C. J., Weber, R. J., and Nenes, A.: Investigation of molar volume and surfactant characteristics of water-soluble organic compounds in biomass burning aerosol, *Atmos. Chem. Phys.*, 8, 799–812, 2008, <http://www.atmos-chem-phys.net/8/799/2008/>. 15599, 15600
- Bachalo, W.: Method for measuring the size and velocity of spheres by dual-beam light-scatter interferometry, *Appl. Optics*, 19, 363–370, 1980. 15609

Title Page

Abstract

Introduction

Conclusions

References

Tables

Figures

I◀

▶I

◀

▶

Back

Close

Full Screen / Esc

Printer-friendly Version

Interactive Discussion



- Bachalo, W. and Houser, M.: Phase Doppler spray analyzer for simultaneous measurements of drop size and velocity distributions, *Opt. Eng.*, 23, 583–590, 1984. 15609
- Broekhuizen, K., Kumar, P., and Abbatt, J.: Partially soluble organics as cloud condensation nuclei: Role of trace soluble and surface active species, *Geophys. Res. Lett.*, 31, 1–5, doi:10.1029/2003GL018203, 2004. 15599, 15600
- 5 Chan, M. N., Kreidenweis, S. M., and Chan, C. K.: Measurements of the hygroscopic and deliquescence properties of organic compounds of different solubilities in water and their relationship with cloud condensation nuclei activities, *Environ. Sci. Technol.*, 42, 3602–3608, doi:10.1021/es7023252, 2008. 15598
- 10 Chang, C. and Franses, E.: Adsorption dynamics of surfactants at the air-water interface - a critical review of mathematical-models, data, and mechanisms, *Colloid Surface A*, 100, 1–45, 1995. 15606
- Chang, C., Wang, N., and Franses, E.: Adsorption dynamics of single and binary surfactants at the air-water interface, *Colloid Surface*, 62, 321–332, 1992. 15606
- 15 Clegg, S., Seinfeld, J., and Brimblecombe, P.: Thermodynamic modelling of aqueous aerosols containing electrolytes and dissolved organic compounds, *J. Aerosol Sci.*, 32, 713–738, 2001. 15605, 15614
- Clegg, S. L., Seinfeld, J. H., and Brimblecombe, P.: A thermodynamic model of the system $\text{H}^+ \text{-NH}_4^+ \text{-Na}^+ \text{-SO}_4^{2-} \text{-NO}_3^- \text{-Cl}^- \text{-H}_2\text{O}$ at 298.15 K, *J. Phys. Chem. A*, 102, 2155–2171, 1998. 15605, 15610
- 20 Clegg, S. L., Seinfeld, J. H., and Brimblecombe, P.: Thermodynamic modelling of aqueous aerosols containing electrolytes and dissolved organic compounds, *J. Aerosol Sci.*, 32, 713–738, 2001. 15605, 15610
- Dinar, E., Taraniuk, I., Graber, E. R., Katsman, S., Moise, T., Anttila, T., Mentel, T. F., and Rudich, Y.: Cloud Condensation Nuclei properties of model and atmospheric HULIS, *Atmos. Chem. Phys.*, 6, 2465–2482, 2006, <http://www.atmos-chem-phys.net/6/2465/2006/>. 15599, 15600
- 25 Dinar, E., Taraniuk, I., Graber, E. R., Anttila, T., Mentel, T. F., and Rudich, Y.: Hygroscopic growth of atmospheric and model humic-like substances, *J. Geophys. Res.-Atmos.*, 112, 1–13, doi:10.1029/2006JD007442, 2007. 15599
- 30 Duplissy, J., Gysel, M., Alfarra, M. R., Dommen, J., Metzger, A., Prevot, A. S. H., Weingartner, E., Laaksonen, A., Raatikainen, T., Good, N., Turner, S. F., McFiggans, G., and Baltensperger, U.: Cloud forming potential of secondary organic aerosol under near atmo-

**High-RH
hygroscopicity**

C. R. Ruehl et al.

Title Page

Abstract

Introduction

Conclusions

References

Tables

Figures

◀

▶

◀

▶

Back

Close

Full Screen / Esc

Printer-friendly Version

Interactive Discussion



- spheric conditions, *Geophys. Res. Lett.*, 35, 1–5, doi:10.1029/2007GL031075, 2008. 15602
- Ellison, G., Tuck, A., and Vaida, V.: Atmospheric processing of organic aerosols, *J. Geophys. Res.-Atmos.*, 104, 11633–11641, 1999. 15607
- Ervens, B., Feingold, G., and Kreidenweis, S.: Influence of water-soluble organic carbon on cloud drop number concentration, *J. Geophys. Res.-Atmos.*, 110, 1–14, doi:10.1029/2004JD005634, 2005. 15599
- Facchini, M., Mircea, M., Fuzzi, S., and Charlson, R.: Cloud albedo enhancement by surface-active organic solutes in growing droplets, *Nature*, 401, 257–259, 1999. 15599
- Facchini, M., Mircea, M., Fuzzi, S., and Charlson, R.: Comments on “Influence of soluble surfactant properties on the activation of aerosol particles containing inorganic solute”, *J. Atmos. Sci.*, 58, 1465–1467, 2001. 15611
- Fitzgerald, J., Hoppel, W., and Vietti, M.: The size and scattering coefficient of urban aerosol-particles at Washington, DC as a function of relative-humidity, *J. Atmos. Sci.*, 39, 1838–1852, 1982. 15602
- Gill, P., Graedel, T., and Weschler, C.: Organic films on atmospheric aerosol-particles, fog droplets, cloud droplets, raindrops, and snowflakes, *Rev. Geophys.*, 21, 903–920, 1983. 15607
- Hanford, K. L., Mitchem, L., Reid, J. P., Clegg, S. L., Topping, D. O., and McFiggans, G. B.: Comparative thermodynamic studies of aqueous glutaric acid, ammonium sulfate and sodium chloride aerosol at high humidity, *J. Phys. Chem. A*, 112, 9413–9422, doi:10.1021/jp802520d, <http://pubs.acs.org/doi/abs/10.1021/jp802520d>, 2008. 15598
- Henning, S., Rosenørn, T., D’Anna, B., Gola, A. A., Svenningsson, B., and Bilde, M.: Cloud droplet activation and surface tension of mixtures of slightly soluble organics and inorganic salt, *Atmos. Chem. Phys.*, 5, 575–582, 2005, <http://www.atmos-chem-phys.net/5/575/2005/>. 15599
- Hings, S. S., Wrobel, W. C., Cross, E. S., Worsnop, D. R., Davidovits, P., and Onasch, T. B.: CCN activation experiments with adipic acid: effect of particle phase and adipic acid coatings on soluble and insoluble particles, *Atmos. Chem. Phys.*, 8, 3735–3748, 2008, <http://www.atmos-chem-phys.net/8/3735/2008/>. 15611
- Hitzenberger, R., Berner, A., Kasper-Giebl, A., Loflund, M., and Puxbaum, H.: Surface tension of Rax cloud water and its relation to the concentration of organic material, *J. Geophys. Res.-Atmos.*, 107, 1–6, doi:10.1029/2002JD002506, 2002. 15599
- Hudson, J. and Da, X.: Volatility and size of cloud condensation nuclei, *J. Geophys. Res.-*

**High-RH
hygroscopicity**

C. R. Ruehl et al.

Title Page

Abstract

Introduction

Conclusions

References

Tables

Figures

◀

▶

◀

▶

Back

Close

Full Screen / Esc

Printer-friendly Version

Interactive Discussion



- Atmos., 101, 4435–4442, 1996. 15601, 15602
- Husar, R. and Shu, W.: Thermal analysis of Los Angeles smog aerosol, *J. Appl. Meteorol.*, 14, 1558–1565, 1975. 15607
- Kiss, G., Tombacz, E., and Hansson, H.: Surface tension effects of humic-like substances in the aqueous extract of tropospheric fine aerosol, *J. Atmos. Chem.*, 50, 279–294, doi:10.1007/s10874-005-5079-5, 2005. 15599
- Kokkola, H., Sorjamaa, R., Peraniemi, A., Raatikainen, T., and Laaksonen, A.: Cloud formation of particles containing humic-like substances, *Geophys. Res. Lett.*, 33, 1–5, doi:10.1029/2006GL026107, 2006. 15600
- Krämer, L., Pöschl, U., and Niessner, R.: Microstructural rearrangement of sodium chloride condensation aerosol particles on interaction with water vapor, *J. Aerosol Sci.*, 31, 673–685, 2000. 15608
- Lewis, E. R.: An examination of Köhler theory resulting in an accurate expression for the equilibrium radius ratio of a hygroscopic aerosol particle valid up to and including relative humidity 100%, *J. Geophys. Res.-Atmos.*, 113, 1–17, doi:10.1029/2007JD008590, 2008. 15598, 15603
- Li, Z., Williams, A., and Rood, M.: Influence of soluble surfactant properties on the activation of aerosol particles containing inorganic solute, *J. Atmos. Sci.*, 55, 1859–1866, 1998. 15600, 15607
- Lima, L. and Synovec, R.: Laser-based dynamic surface-tension detection for liquid-chromatography by probing a repeating drop radius, *J. Chromatogr. A*, 691, 195–204, 1995. 15599
- Loglio, G., Pandolfini, P., Tesei, U., and Noskov, B.: Measurements of interfacial properties with the axisymmetric bubble-shape analysis technique: effects of vibrations, *Colloid Surface A*, 143, 301–310, 1998. 15599
- Lohmann, U. and Leck, C.: Importance of submicron surface-active organic aerosols for pristine Arctic clouds, *Tellus B*, 57, 261–268, 2005. 15599
- Matubayasi, N. and Nishiyama, A.: Thermodynamic quantities of surface formation of aqueous electrolyte solutions VI. Comparison with typical nonelectrolytes, sucrose and glucose, *J. Colloid Interf. Sci.*, 298, 910–913, doi:10.1016/j.jcis.2006.01.008, 2006. 15613, 15618
- Mircea, M., Facchini, M. C., Decesari, S., Cavalli, F., Emblico, L., Fuzzi, S., Vestin, A., Rissler, J., Swietlicki, E., Frank, G., Andreae, M. O., Maenhaut, W., Rudich, Y., and Artaxo, P.: Importance of the organic aerosol fraction for modeling aerosol hygroscopic growth and activation:

**High-RH
hygroscopicity**

C. R. Ruehl et al.

Title Page

Abstract

Introduction

Conclusions

References

Tables

Figures

◀

▶

◀

▶

Back

Close

Full Screen / Esc

Printer-friendly Version

Interactive Discussion



**High-RH
hygroscopicity**

C. R. Ruehl et al.

Title Page

Abstract

Introduction

Conclusions

References

Tables

Figures

◀

▶

◀

▶

Back

Close

Full Screen / Esc

Printer-friendly Version

Interactive Discussion



a case study in the Amazon Basin, *Atmos. Chem. Phys.*, 5, 3111–3126, 2005,

<http://www.atmos-chem-phys.net/5/3111/2005/>. 15599

Nakahara, H., Shibata, O., Rusdi, M., and Moroi, Y.: Examination of surface adsorption of soluble surfactants by surface potential measurement at the air/solution interface, *J. Phys. Chem. C*, 112, 6398–6403, doi:10.1021/jp7108169, 2008. 15617

Niedermeier, D., Wex, H., Voigtländer, J., Stratmann, F., Brüggemann, E., Kiselev, A., Henk, H., and Heintzenberg, J.: LACIS-measurements and parameterization of sea-salt particle hygroscopic growth and activation, *Atmos. Chem. Phys.*, 8, 579–590, 2008,

<http://www.atmos-chem-phys.net/8/579/2008/>. 15598

Petters, M. D. and Kreidenweis, S. M.: A single parameter representation of hygroscopic growth and cloud condensation nucleus activity, *Atmos. Chem. Phys.*, 7, 1961–1971, 2007,

<http://www.atmos-chem-phys.net/7/1961/2007/>. 15601, 15602

Prosser, A. and Franses, E.: Adsorption and surface tension of ionic surfactants at the air-water interface: review and evaluation of equilibrium models, *Colloid Surface A*, 178, 1–40, 2001.

15606

Rissman, T., Nenes, A., and Seinfeld, J.: Chemical amplification (or dampening) of the Twomey effect: Conditions derived from droplet activation theory, *J. Atmos. Sci.*, 61, 919–930, 2004.

15599

Roberts, G. and Nenes, A.: A continuous-flow streamwise thermal-gradient CCN chamber for atmospheric measurements, *Aerosol Sci. Tech.*, 39, 206–221, 2005. 15609

Ruehl, C. R., Chuang, P. Y., and Nenes, A.: How quickly do cloud droplets form on atmospheric particles?, *Atmos. Chem. Phys.*, 8, 1043–1055, 2008, <http://www.atmos-chem-phys.net/8/1043/2008/>. 15609

Russell, L., Maria, S., and Myneni, S.: Mapping organic coatings on atmospheric particles, *Geophys. Res. Lett.*, 29, 1–4, doi:10.1029/2002GL014874, 2002. 15607

Saxena, P. and Hildemann, L.: Water-soluble organics in atmospheric particles: A critical review of the literature and application of thermodynamics to identify candidate compounds, *J. Atmos. Chem.*, 24, 57–109, 1996. 15614

Seidl, W. and Hanel, G.: Surface-active substances on rainwater and atmospheric particles, *Pure Appl. Geophys.*, 121, 1077–1093, 1983. 15599

Shulman, M., Jacobson, M., Carlson, R., Synovec, R., and Young, T.: Dissolution behavior and surface tension effects of organic compounds in nucleating cloud droplets, *Geophys. Res. Lett.*, 23, 277–280, 1996. 15599

**High-RH
hygroscopicity**

C. R. Ruehl et al.

Title Page

Abstract

Introduction

Conclusions

References

Tables

Figures

◀

▶

◀

▶

Back

Close

Full Screen / Esc

Printer-friendly Version

Interactive Discussion



- 5 Sorjamaa, R. and Laaksonen, A.: The influence of surfactant properties on critical supersaturations of cloud condensation nuclei, *J. Aerosol Sci.*, 37, 1730–1736, doi:10.1016/j.jaerosci.2006.07.004, 2006. 15600
- 5 Sorjamaa, R., Svenningsson, B., Raatikainen, T., Henning, S., Bilde, M., and Laaksonen, A.: The role of surfactants in Köhler theory reconsidered, *Atmos. Chem. Phys.*, 4, 2107–2117, 2004, <http://www.atmos-chem-phys.net/4/2107/2004/>. 15600, 15607
- 10 Stokes, R. H. and Robinson, R. A.: Interactions in aqueous nonelectrolyte solutions. I. Solute-solvent equilibria, *J. Phys. Chem.*, 70, 2126–2131, doi:10.1021/j100879a010, <http://pubs.acs.org/doi/abs/10.1021/j100879a010>, 1966. 15605, 15614
- 10 Szyskowski, B.: Experimentelle studien über kapillare eigenschaften der wässrigen lösungen von fettsauren, *Z. Phys. Chem.*, 64, 385–414, 1908. 15603, 15606
- Tabazadeh, A.: Organic aggregate formation in aerosols and its impact on the physicochemical properties of atmospheric particles., *Atmos. Environ.*, 39, 5472–5480, doi:10.1016/j.atmosenv.2005.05.045, 2005. 15600, 15613
- 15 Taraniuk, I., Kostinski, A. B., and Rudich, Y.: Enrichment of surface-active compounds in coalescing cloud drops, *Geophys. Res. Lett.*, 35, 1–5, doi:10.1029/2008GL034973, 2008. 15599
- Tervahattu, H., Hartonen, K., Kerminen, V., Kupiainen, K., Aarnio, P., Koskentalo, T., Tuck, A., and Vaida, V.: New evidence of an organic layer on marine aerosols, *J. Geophys. Res.-Atmos.*, 107, 1–8, doi:10.1029/2000JD000282, 2002. 15607
- 20 Textor, C., Schulz, M., Guibert, S., Kinne, S., Balkanski, Y., Bauer, S., Bernsten, T., Berglen, T., Boucher, O., Chin, M., Dentener, F., Diehl, T., Easter, R., Feichter, H., Fillmore, D., Ghan, S., Ginoux, P., Gong, S., Grini, A., Hendricks, J., Horowitz, L., Huang, P., Isaksen, I., Iversen, I., Kloster, S., Koch, D., Kirkevåg, A., Kristjansson, J. E., Krol, M., Lauer, A., Lamarque, J. F., Liu, X., Montanaro, V., Myhre, G., Penner, J., Pitari, G., Reddy, S., Seland, Ø., Stier, P., Takemura, T., and Tie, X.: Analysis and quantification of the diversities of aerosol life cycles within AeroCom, *Atmos. Chem. Phys.*, 6, 1777–1813, 2006, <http://www.atmos-chem-phys.net/6/1777/2006/>. 15597
- 25 Timmermans, J.: The Physico-chemical constants of binary systems in concentrated solutions, Vol. 4, Interscience Publishers, New York, 1960. 15610
- 30 Topping, D. O., McFiggans, G. B., Kiss, G., Varga, Z., Facchini, M. C., Decesari, S., and Mircea, M.: Surface tensions of multi-component mixed inorganic/organic aqueous systems of atmospheric significance: measurements, model predictions and importance for cloud activation predictions, *Atmos. Chem. Phys.*, 7, 2371–2398, 2007, <http://www.atmos-chem-phys.net/7/2371/2007/>. 15600, 15607

phys.net/7/2371/2007/. 15600

Vanhanen, J., Hyvärinen, A.-P., Anttila, T., Raatikainen, T., Viisanen, Y., and Lihavainen, H.: Ternary solution of sodium chloride, succinic acid and water; surface tension and its influence on cloud droplet activation, *Atmos. Chem. Phys.*, 8, 4595–4604, 2008, <http://www.atmos-chem-phys.net/8/4595/2008/>. 15599

Varga, Z., Kiss, G., and Hansson, H.-C.: Modelling the cloud condensation nucleus activity of organic acids on the basis of surface tension and osmolality measurements, *Atmos. Chem. Phys.*, 7, 4601–4611, 2007, <http://www.atmos-chem-phys.net/7/4601/2007/>. 15599

Wex, H., Petters, M. D., Carrico, C. M., Hallbauer, E., Massling, A., McMeeking, G. R., Poulain, L., Wu, Z., Kreidenweis, S. M., and Stratmann, F.: Towards closing the gap between hygroscopic growth and activation for secondary organic aerosol: Part 1 – Evidence from measurements, *Atmos. Chem. Phys.*, 9, 3987–3997, 2009, <http://www.atmos-chem-phys.net/9/3987/2009/>. 15598, 15600

Wex, H., Kiselev, A., Stratmann, F., Zoboki, J., and Brechtel, F.: Measured and modeled equilibrium sizes of NaCl and (NH₄)₂SO₄ particles at relative humidities up to 99.1%, *J. Geophys. Res.-Atmos.*, 110, 1–9, doi:10.1029/2004JD005507, 2005. 15598, 15615

Wex, H., Hennig, T., Salma, I., Ocskay, R., Kiselev, A., Henning, S., Massling, A., Wiedensohler, A., and Stratmann, F.: Hygroscopic growth and measured and modeled critical super-saturations of an atmospheric HULIS sample, *Geophys. Res. Lett.*, 34, 1–5, doi:10.1029/2006GL028260, 2007. 15601, 15602

Widera, B., Neueder, R., and Kunz, W.: Vapor pressures and osmotic coefficients of aqueous solutions of SDS, C(6)TAB, and C(8)TAB at 25 degrees C, *Langmuir*, 19, 8226–8229, doi:10.1021/la034714+, 2003. 15611

Zelenyuk, A., Cai, Y., and Imre, D.: From agglomerates of spheres to irregularly shaped particles: Determination of dynamic shape factors from measurements of mobility and vacuum aerodynamic diameters, *Aerosol Sci. Tech.*, 40, 197–217, doi:10.1080/02786820500529406, 2006. 15608

Ziese, M., Wex, H., Nilsson, E., Salma, I., Ocskay, R., Hennig, T., Massling, A., and Stratmann, F.: Hygroscopic growth and activation of HULIS particles: experimental data and a new iterative parameterization scheme for complex aerosol particles, *Atmos. Chem. Phys.*, 8, 1855–1866, 2008,

<http://www.atmos-chem-phys.net/8/1855/2008/>. 15598

ACPD

9, 15595–15640, 2009

High-RH hygroscopicity

C. R. Ruehl et al.

Title Page

Abstract

Introduction

Conclusions

References

Tables

Figures

◀

▶

◀

▶

Back

Close

Full Screen / Esc

Printer-friendly Version

Interactive Discussion



High-RH hygroscopicity

C. R. Ruehl et al.

Table 1. High-RH hygroscopicity (κ_{obs}) of the NaCl reference and six other compounds. Also κ_{ideal} , the theoretical value at RH=100% assuming an ideal solution, infinite solubility, and either complete dissociation (NaCl, AS, and SDS) or no dissociation (malonic and adipic acids, glucose, and sucrose). Also listed are the slopes (m) and p -values for linear regressions of κ onto RH. p -values under 5% are in boldface.

	κ_{obs}	κ_{ideal}	n	m [% % ⁻¹]	p
NaCl	1.27*±0.11	1.33	77	-1.2	0.84
AS	0.572±0.074	0.72	54	20	0.068
malonic acid	0.291±0.057	0.28	35	46	0.009
adipic acid	0.185±0.040	0.168	13	100	0.050
glucose	0.165±0.033	0.154	20	63	0.13
SDS	0.134±0.029	0.147	53	2.72	0.86
sucrose	0.112±0.020	0.084	27	-54	0.028

* This value was fixed in the RH calibration.

[Title Page](#)
[Abstract](#)
[Introduction](#)
[Conclusions](#)
[References](#)
[Tables](#)
[Figures](#)
[I◀](#)
[▶I](#)
[◀](#)
[▶](#)
[Back](#)
[Close](#)
[Full Screen / Esc](#)
[Printer-friendly Version](#)
[Interactive Discussion](#)


High-RH hygroscopicity

C. R. Ruehl et al.

Table 2. Slopes (m) and significance (p -value) of trends in both hygroscopicity parameters (κ and δ) with D_{wet} . p -values under 5% are in boldface.

	m_{κ} [% μm^{-1}]	m_{δ} [% μm^{-1}]	p_{κ}	p_{δ}
NaCl	3.3	-8.1	0.13	0.26
AS	4.5	-0.5	0.42	0.98
malonic acid	41	-120	0.001	0.014
adipic acid	47	-27	0.015	0.52
glucose	42	-76	0.033	0.085
SDS	65	-210	1×10^{-6}	1×10^{-6}
sucrose	22	-100	0.26	0.051

[Title Page](#)
[Abstract](#)
[Introduction](#)
[Conclusions](#)
[References](#)
[Tables](#)
[Figures](#)
[I◀](#)
[▶I](#)
[◀](#)
[▶](#)
[Back](#)
[Close](#)
[Full Screen / Esc](#)
[Printer-friendly Version](#)
[Interactive Discussion](#)


High-RH
hygroscopicity

C. R. Ruehl et al.

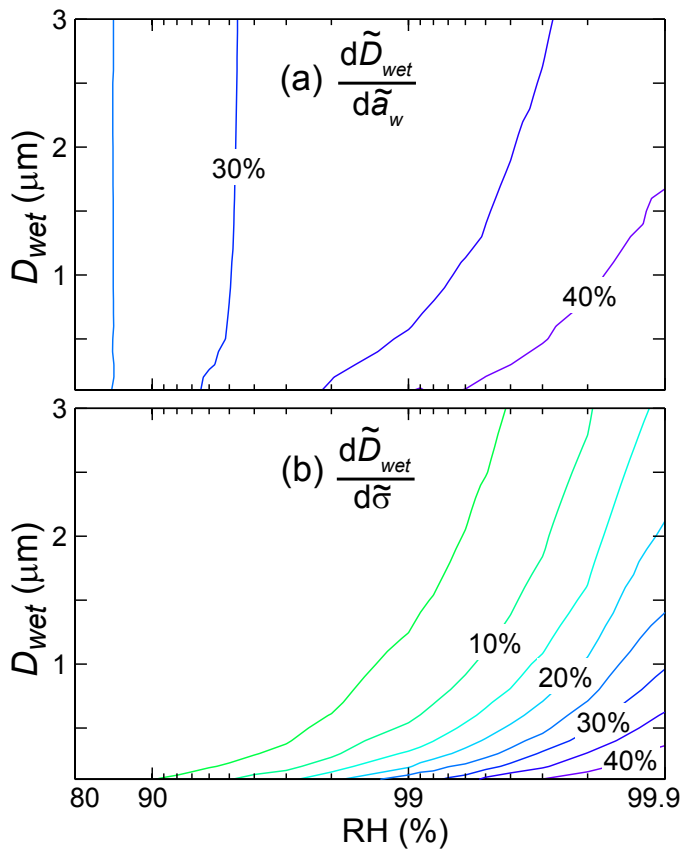


Fig. 1. Sensitivity of D_{wet} to changes in (a) water activity and (b) surface tension. Contour interval is 5%.

[Title Page](#)[Abstract](#)[Introduction](#)[Conclusions](#)[References](#)[Tables](#)[Figures](#)[I◀](#)[▶I](#)[◀](#)[▶](#)[Back](#)[Close](#)[Full Screen / Esc](#)[Printer-friendly Version](#)[Interactive Discussion](#)

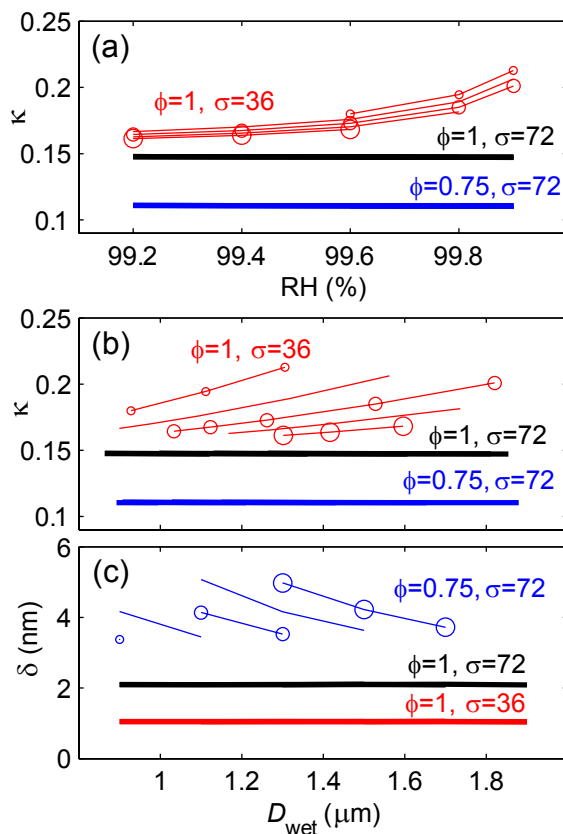


Fig. 2. Theoretical variation of κ with both (a) RH and (b) D_{wet} , and of (c) δ with D_{wet} . Black curves are for ideal ($\phi=1$) sodium dodecyl sulfate (SDS) solution droplet with a surface tension (σ) of water, red curves assume σ is reduced by half, and blue curves assume $\phi=0.75$. Sensitivity of κ and δ to dry particle size is indicated by symbol size for pure SDS with D_{dry} used in experiments (0.3 to 0.5 μm).

Title Page

Abstract

Introduction

Conclusions

References

Tables

Figures

◀

▶

◀

▶

Back

Close

Full Screen / Esc

Printer-friendly Version

Interactive Discussion



High-RH
hygroscopicity

C. R. Ruehl et al.

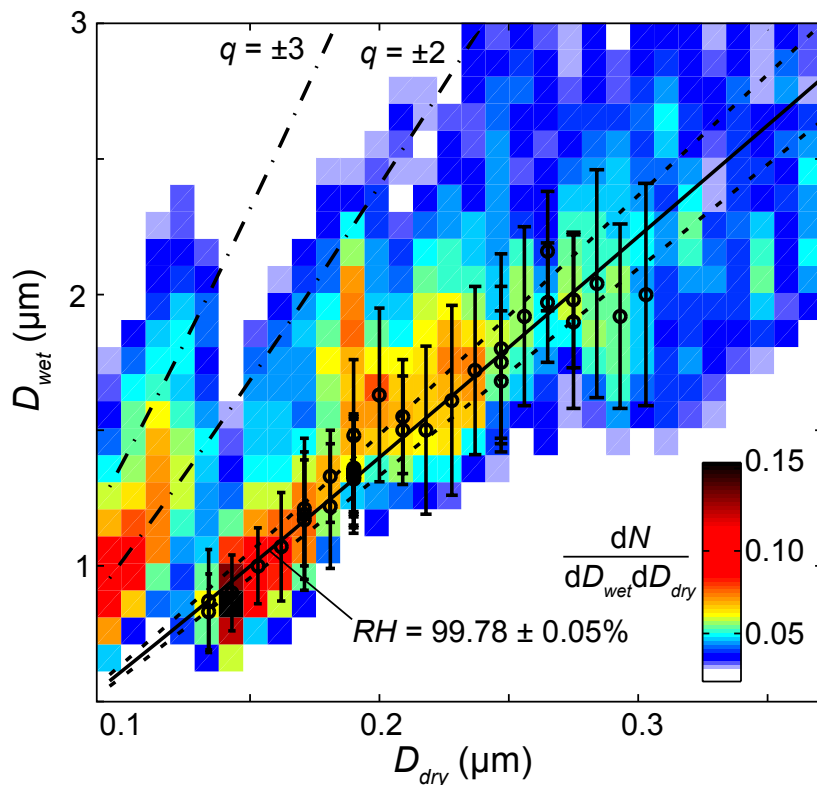


Fig. 3. D_{wet} spectra (color), vs. D_{dry} of NaCl particles. Includes D_{wet} fit peaks (circles) and standard deviations (error bars) used to determine RH, along with a solid line for the best fit RH, dotted lines indicating the precision of the RH calculation, and dash-dot lines representing multiply-charged particles selected by the DMA.

[Title Page](#)[Abstract](#)[Introduction](#)[Conclusions](#)[References](#)[Tables](#)[Figures](#)[◀](#)[▶](#)[◀](#)[▶](#)[Back](#)[Close](#)[Full Screen / Esc](#)[Printer-friendly Version](#)[Interactive Discussion](#)

High-RH
hygroscopicity

C. R. Ruehl et al.

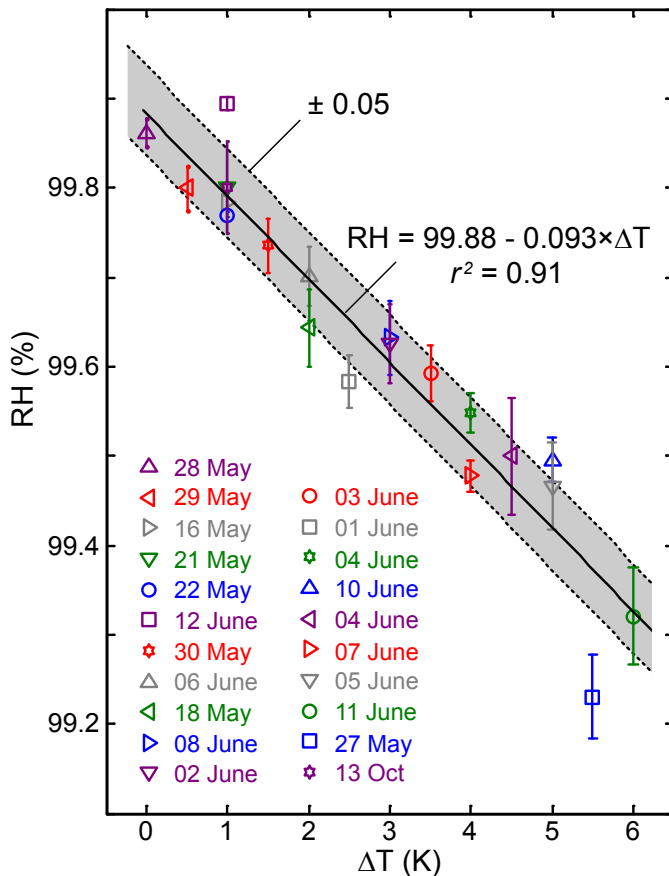


Fig. 4. RH vs. ΔT , with RH derived from observed D_{wet} of NaCl solution droplets, assuming $\kappa = 1.24$ to 1.27 (based on the E-AIM model) and shape-corrected diameter ($\chi = 1.08$).

Title Page

Abstract

Introduction

Conclusions

References

Tables

Figures

◀

▶

◀

▶

Back

Close

Full Screen / Esc

Printer-friendly Version

Interactive Discussion



High-RH
hygroscopicity

C. R. Ruehl et al.

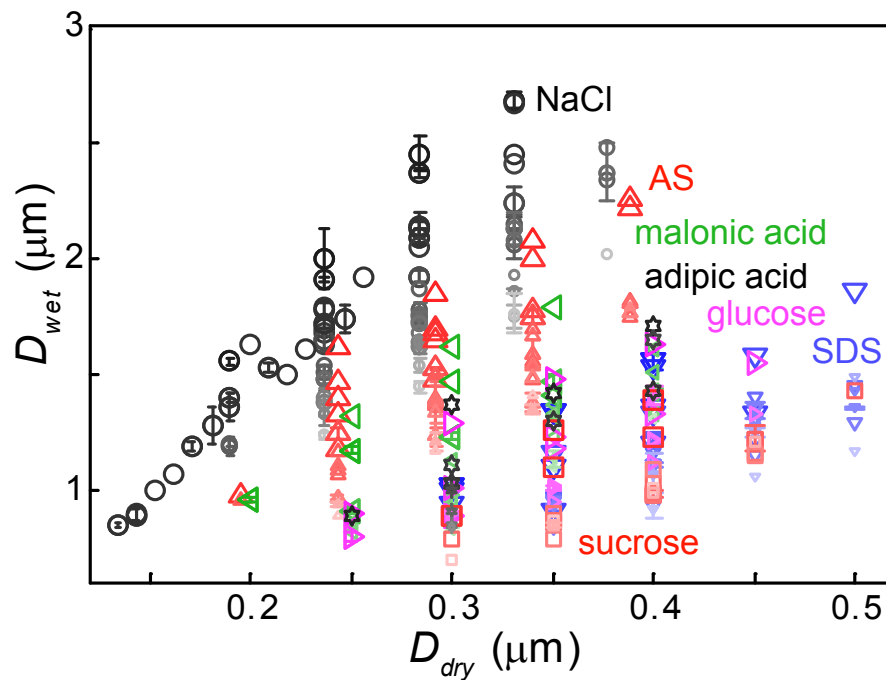


Fig. 5. D_{wet} vs. D_{dry} for all measurements. With duplicate measurement error bars, and marker size and color fade indicating RH. For NaCl, these are the same data as in Fig. 4.

[Title Page](#)[Abstract](#)[Introduction](#)[Conclusions](#)[References](#)[Tables](#)[Figures](#)[◀](#)[▶](#)[◀](#)[▶](#)[Back](#)[Close](#)[Full Screen / Esc](#)[Printer-friendly Version](#)[Interactive Discussion](#)

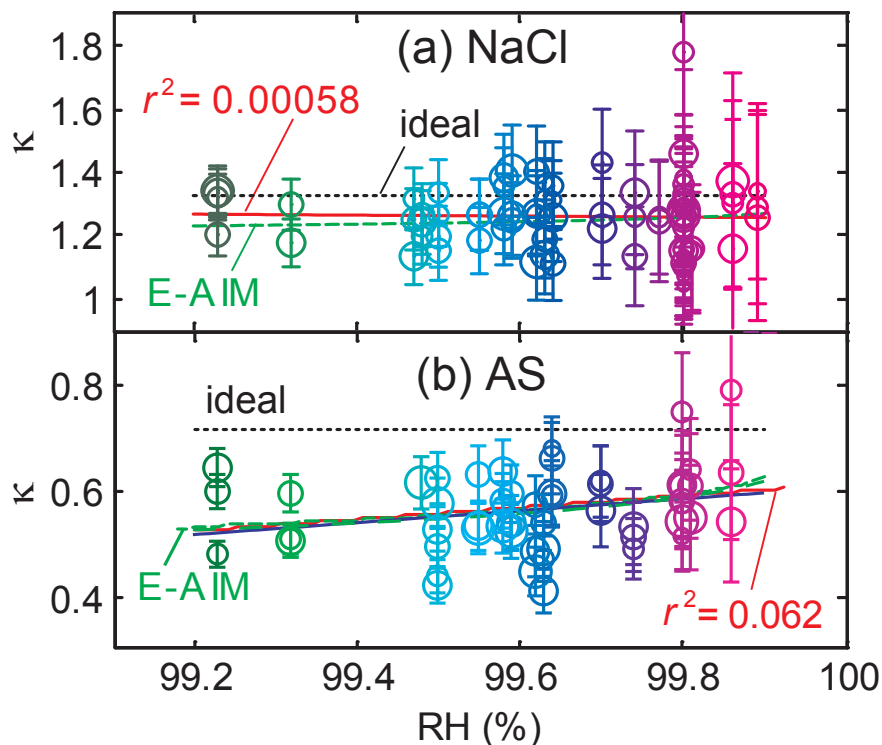


Fig. 6. Hygroscopicity (κ) of **(a)** NaCl and **(b)** AS vs. RH. With linear regressions (red solid lines), data from macroscopic solutions as represented in the E-AIM model (green dashed lines), and values for ideal solutions with the surface tension of water (black dotted lines). Error bars indicate the error in κ associated with an error in RH of $\pm 0.5\%$ (absolute).

[Title Page](#)[Abstract](#)[Introduction](#)[Conclusions](#)[References](#)[Tables](#)[Figures](#)[◀](#)[▶](#)[◀](#)[▶](#)[Back](#)[Close](#)[Full Screen / Esc](#)[Printer-friendly Version](#)[Interactive Discussion](#)

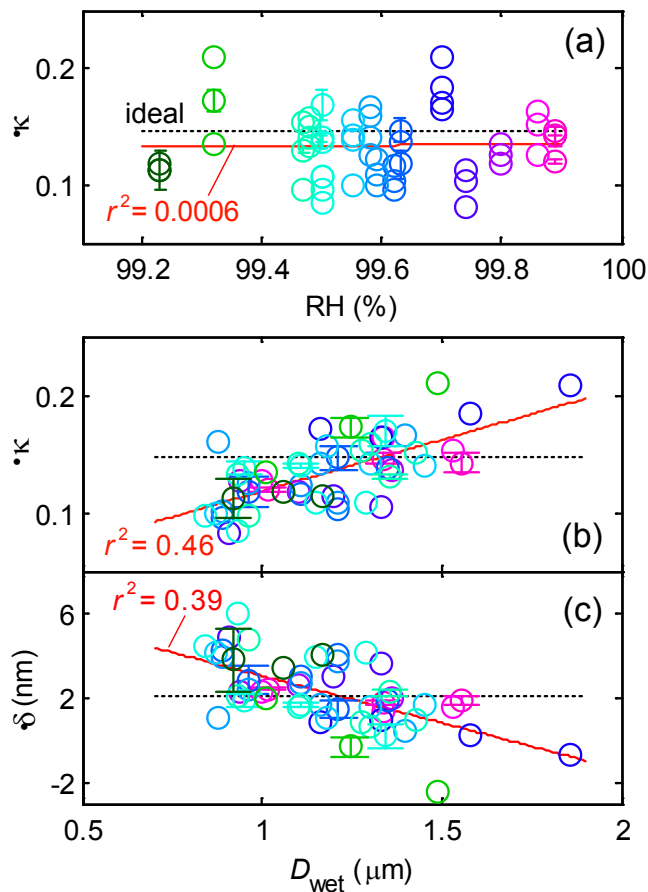


Fig. 7. SDS hygroscopicity hygroscopicity, with linear regressions (red solid lines) and values for ideal solutions with the surface tension of water (black dotted lines). Error bars indicate duplicate D_{wet} standard deviations. **(a)** κ vs. RH. **(b)** κ vs. D_{wet} . **(c)** δ vs. D_{wet} .

[Title Page](#)[Abstract](#)[Introduction](#)[Conclusions](#)[References](#)[Tables](#)[Figures](#)[◀](#)[▶](#)[◀](#)[▶](#)[Back](#)[Close](#)[Full Screen / Esc](#)[Printer-friendly Version](#)[Interactive Discussion](#)

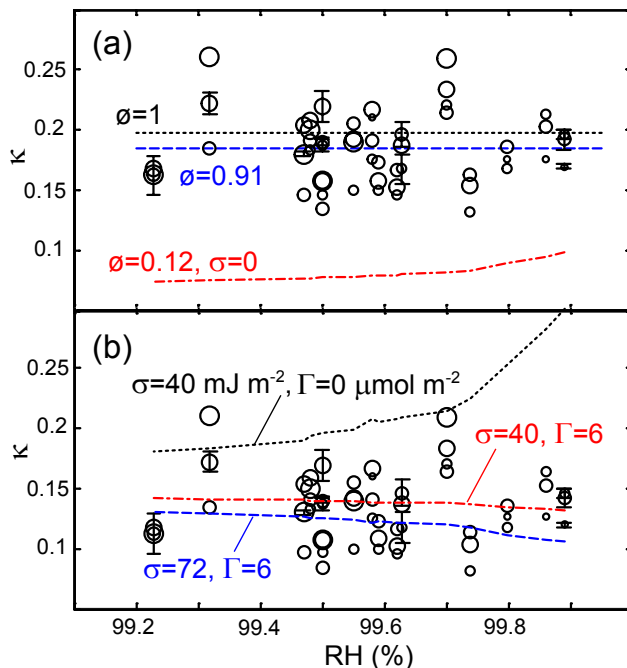


Fig. 8. Theoretical variation in SDS κ with RH (lines) for several cases, with observations (black circles). **(a)** Predicted κ for three cases: an ideal solution droplet with the surface tension of pure water (black dotted line), a droplet with ϕ set to match average observed κ and the surface tension of pure water (blue dashed line), and a droplet with ϕ limited by micellization and a surface tension of zero (red dash-dot line). Even when $\sigma=0$, micellization would result in droplets with $\kappa \sim \frac{1}{2}$ of the observed values. **(b)** Three cases related to surface activity: only surface tension reduction ($\sigma=40 \text{ mJ m}^{-2}$), only surface partitioning and $\Gamma=6 \text{ } \mu\text{mol m}^{-2}$ (dashed blue line), and both. When both surface effects are considered, they tend to cancel out in terms of their influence on κ vs. RH.

Title Page

Abstract

Introduction

Conclusions

References

Tables

Figures

◀

▶

◀

▶

Back

Close

Full Screen / Esc

Printer-friendly Version

Interactive Discussion



High-RH
hygroscopicity

C. R. Ruehl et al.

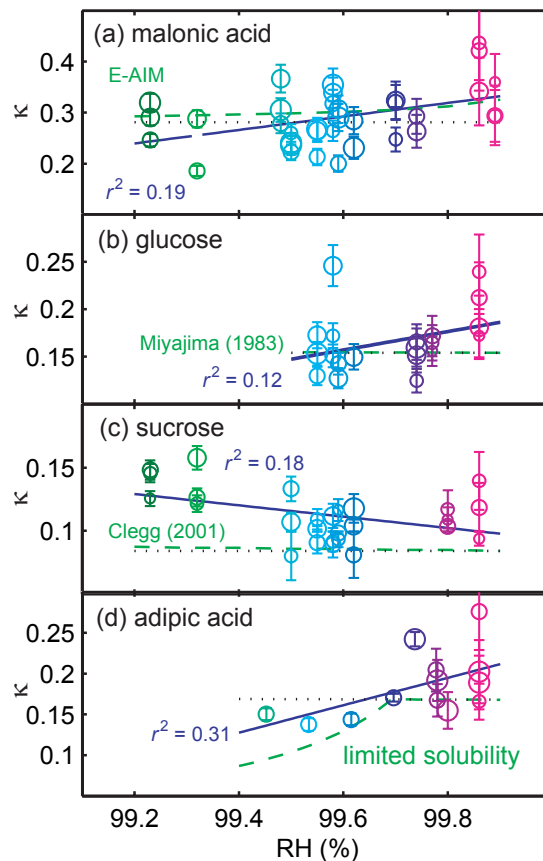


Fig. 9. Organic hygroscopicity (κ) vs. RH. With linear regressions (red solid lines), values for ideal solutions with the surface tension of water (black dotted lines), and theoretical values (green dashed lines). Error bars indicate the error in κ associated with an error in RH of $\pm 0.5\%$ (absolute). **(a)** malonic acid. **(b)** glucose. **(c)** sucrose. **(d)** adipic acid.

Title Page

Abstract

Introduction

Conclusions

References

Tables

Figures

◀

▶

◀

▶

Back

Close

Full Screen / Esc

Printer-friendly Version

Interactive Discussion



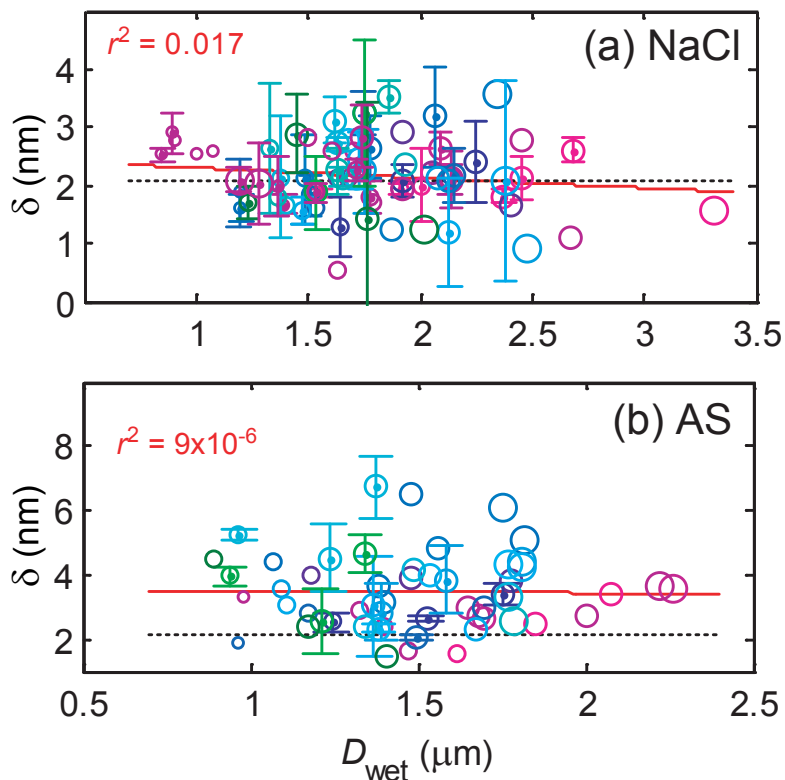


Fig. 10. Hygroscopicity (δ) of **(a)** NaCl and **(b)** AS vs. D_{wet} . With linear regressions (red solid lines) and values for ideal solutions with the surface tension of water (black dotted lines). Error bars indicate duplicate D_{wet} standard deviations.

[Title Page](#)[Abstract](#)[Introduction](#)[Conclusions](#)[References](#)[Tables](#)[Figures](#)[◀](#)[▶](#)[◀](#)[▶](#)[Back](#)[Close](#)[Full Screen / Esc](#)[Printer-friendly Version](#)[Interactive Discussion](#)

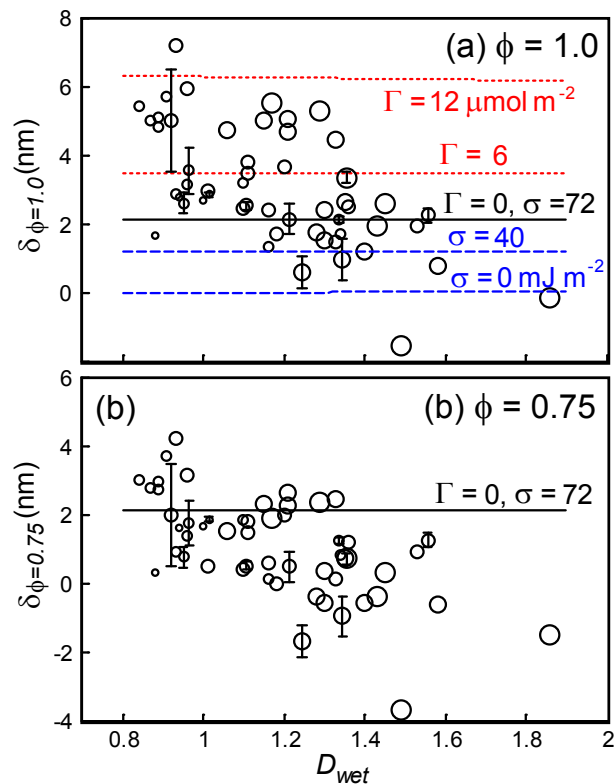


Fig. 11. (a) Observed SDS δ , and predicted δ under several assumptions regarding surface activity. Surface partitioning (i.e., $\Gamma > 0$) tends to decrease hygroscopicity, or increase δ , while surface tension reduction ($\sigma < 72 \text{ mJ m}^{-2}$) has the opposite effect. (b) Observed δ with all calculations of δ made assuming $\phi = 0.75$. This results in a downward shift in all δ , but has only a minor effect on the trend in δ with D_{wet} .

[Title Page](#)
[Abstract](#)
[Introduction](#)
[Conclusions](#)
[References](#)
[Tables](#)
[Figures](#)
[◀](#)
[▶](#)
[◀](#)
[▶](#)
[Back](#)
[Close](#)
[Full Screen / Esc](#)
[Printer-friendly Version](#)
[Interactive Discussion](#)


High-RH
hygroscopicity

C. R. Ruehl et al.

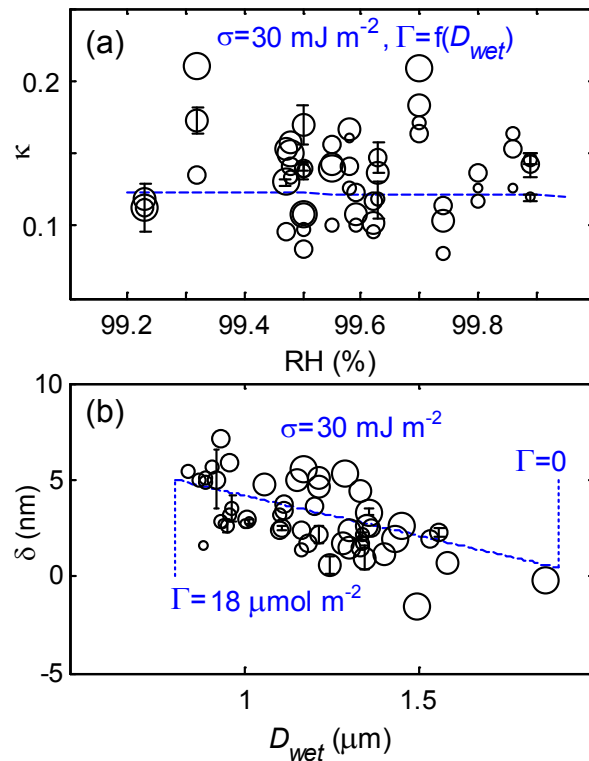


Fig. 12. Observed trends hygroscopicity with RH and D_{wet} (black circles), and predictions (blue dashed lines) assuming $\phi=1$, and that as D_{wet} increases from 0.8 to 1.8 μm , Γ decreases linearly from 18 to 0 $\mu\text{mol m}^{-2}$. σ is held constant at 30 mJ m^{-2} .

[Title Page](#)[Abstract](#)[Introduction](#)[Conclusions](#)[References](#)[Tables](#)[Figures](#)[◀](#)[▶](#)[◀](#)[▶](#)[Back](#)[Close](#)[Full Screen / Esc](#)[Printer-friendly Version](#)[Interactive Discussion](#)

High-RH
hygroscopicity

C. R. Ruehl et al.

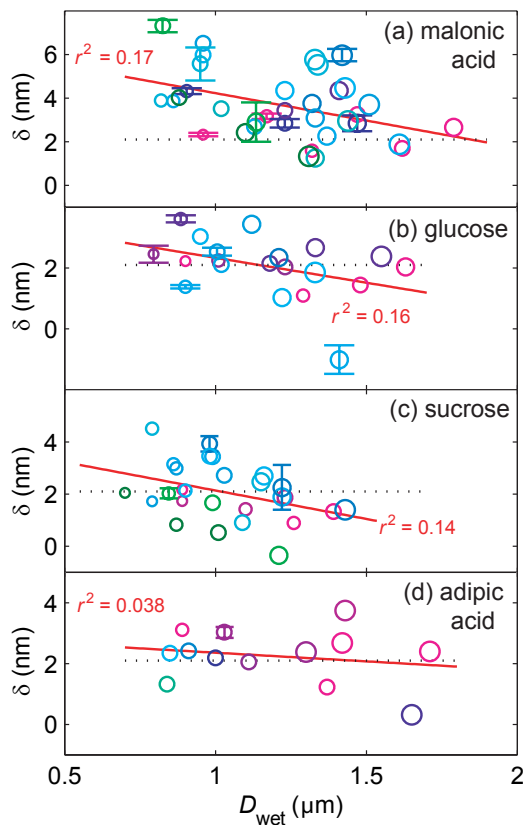


Fig. 13. Organic hygroscopicity (δ) vs. D_{wet} . With linear regressions (red solid lines), and values for ideal solutions with the surface tension of water (black dotted lines). Error bars, symbol size, and color indicate duplicate D_{wet} standard deviations, dry diameter, and RH, respectively. **(a)** malonic acid. **(b)** glucose. **(c)** sucrose. **(d)** adipic acid.

[Title Page](#)[Abstract](#)[Introduction](#)[Conclusions](#)[References](#)[Tables](#)[Figures](#)[◀](#)[▶](#)[◀](#)[▶](#)[Back](#)[Close](#)[Full Screen / Esc](#)[Printer-friendly Version](#)[Interactive Discussion](#)